University of Liège
Aerospace & Mechanical Engineering Department

Computational homogenization of cellular materials capturing micro-buckling, macro-localization and size effects

Van Dung NGUYEN
vandung.nguyen@ulg.ac.be

March 2014

- Cellular materials: “a cellular solid is one made up of an interconnected network of solid struts or plates which form the edges and faces of cells”

(Gibson & Ashby 1999)

- Classification based on the topology
  - Honeycombs: 2-dimensional arrays of polygons (e.g. Bee hexagons)
  - Foams: 3-dimensional network of cell edges and cell faces
    - Network of cell edges →open-cell foams
    - Network of cell faces →closed-cell foams
    - Partly open- & partly closed-cell foams

- Man-made cellular materials

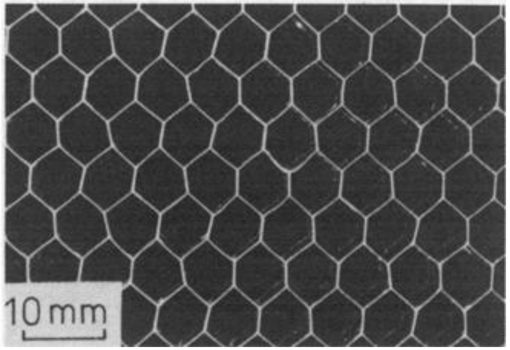

Aluminum honeycomb

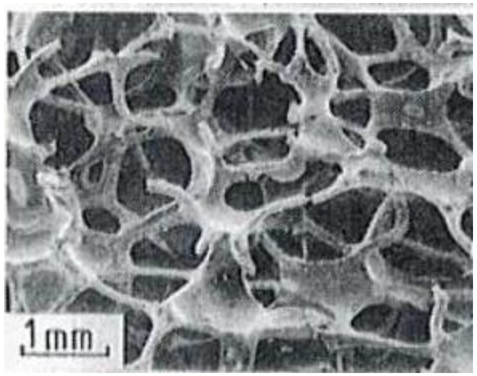

Open-cell nickel foam

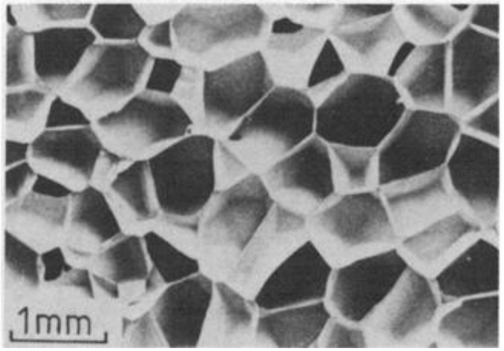

Closed-cell polyurethane foam

- Natural cellular materials

(a) cork
(b) balsa
(c) sponge
(d) trabecular bone
(e) coral
(f) cuttlefish bone
(g) iris leaf
(h) plant stalk

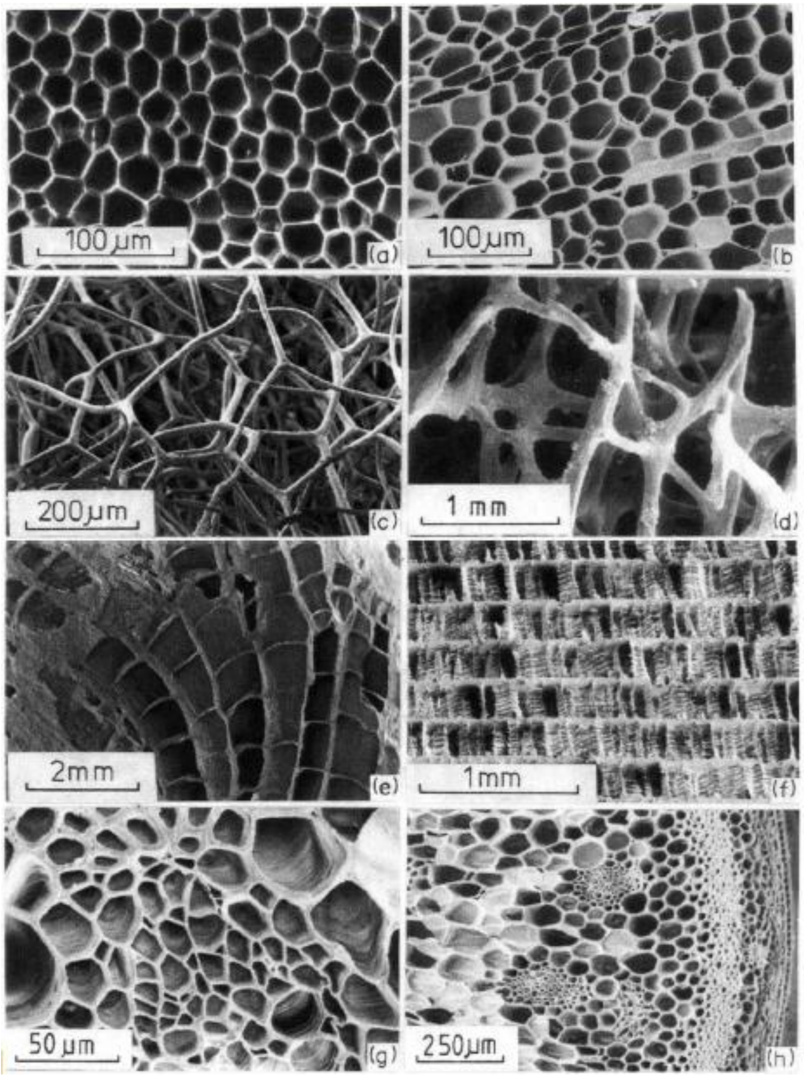

(Gibson & Ashby 1999)

Introduction

- Cellular materials are used in many applications
  - Light weight structures
  - Energy absorption
  - Packaging
  - Sound absorption
  - Thermal insulation
  - Etc.




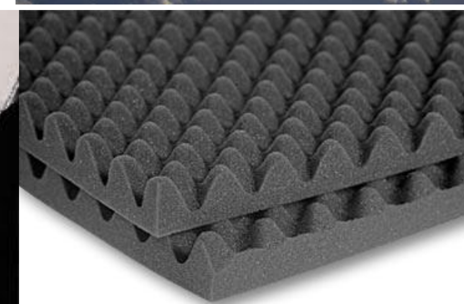




Introduction

- ARC (Action de Recherche concertée) project

“From imaging to geometrical modeling of complex micro-structured materials: Bridging computational engineering and material science”

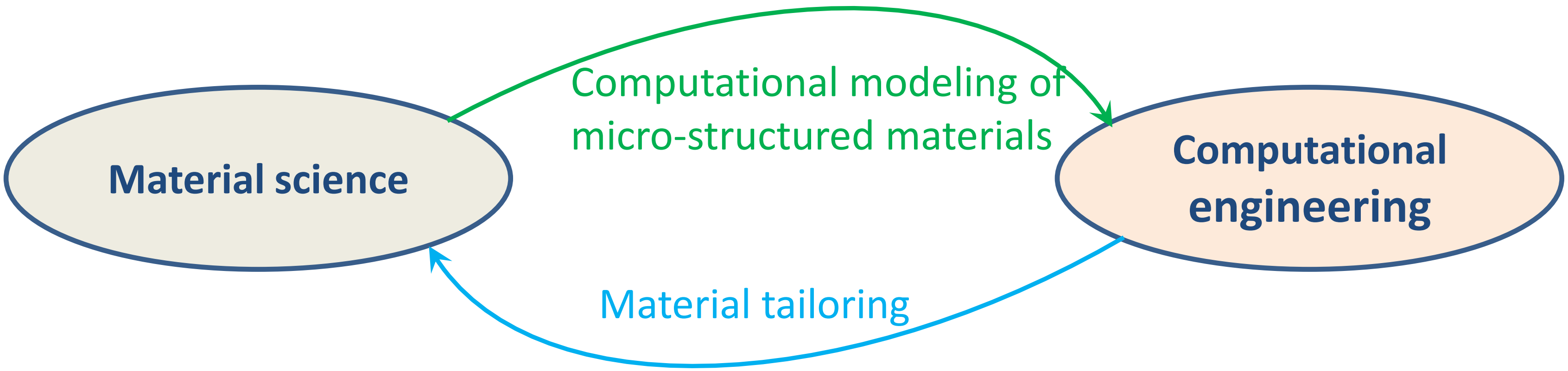

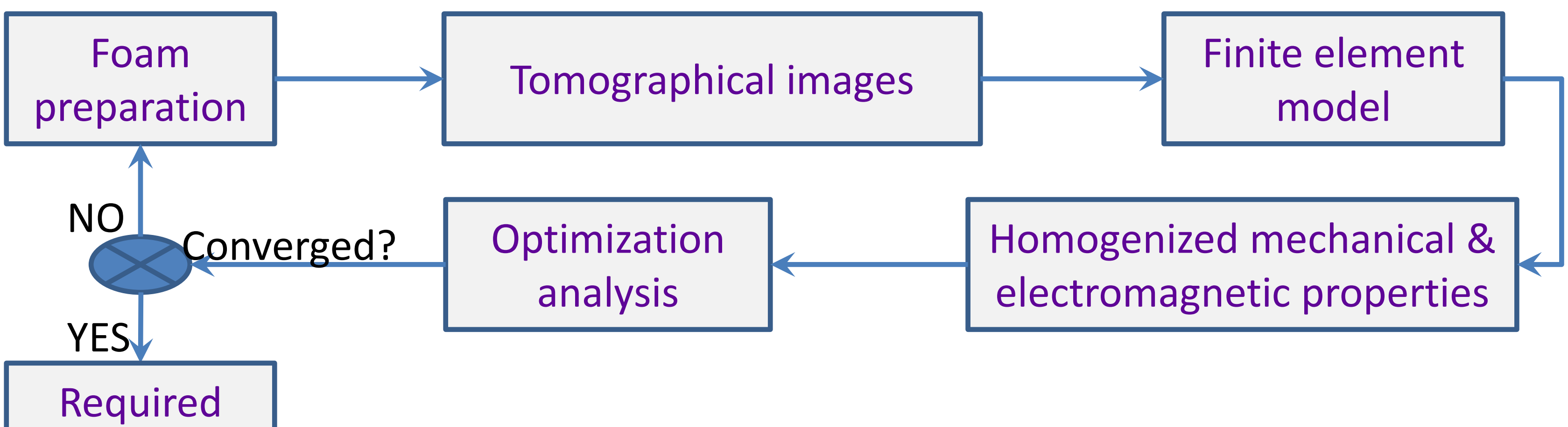

An optimization procedure for “material tailoring”

- Mechanical behavior of cellular materials
  - Buckling of thin components (cell struts, cell faces) can occur under compression loads leading to macroscopic localization

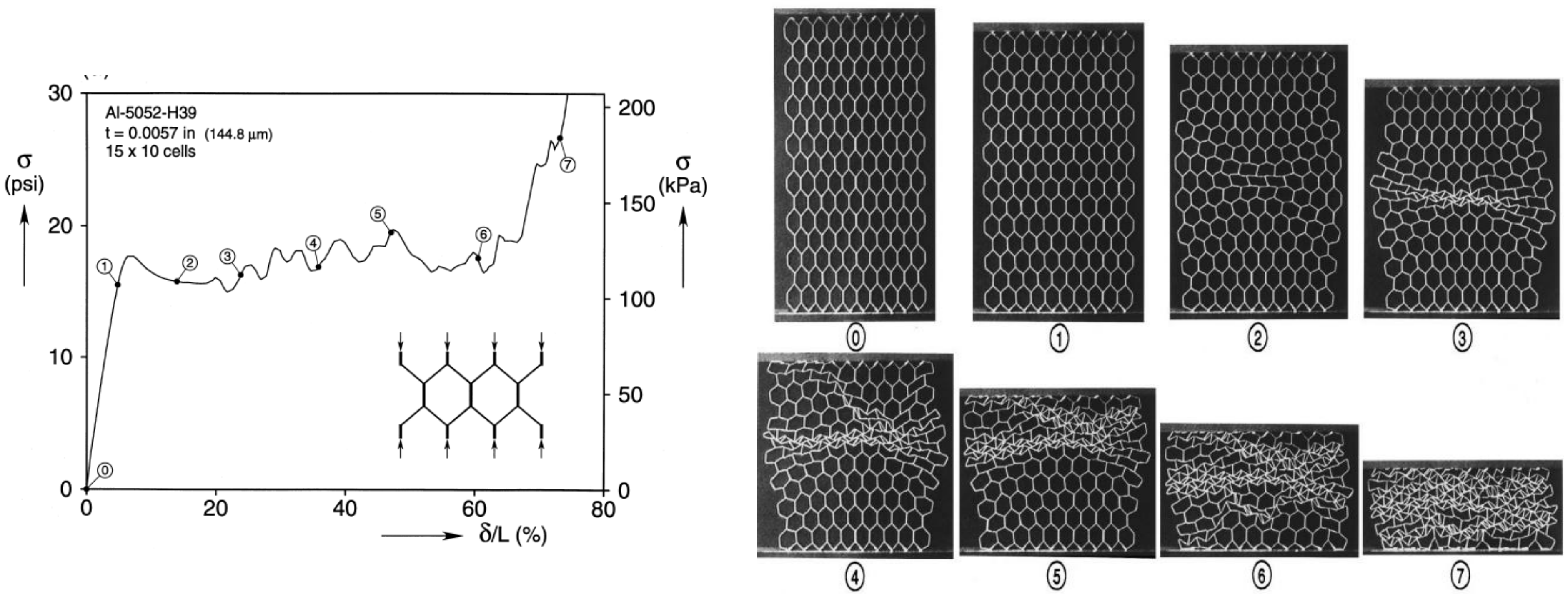

Force-displacement crushing response of aluminum honeycomb
(Experimental data from Papka & Kyriakides 1999)

- Mechanical behavior of cellular materials (2)
  - Size effect

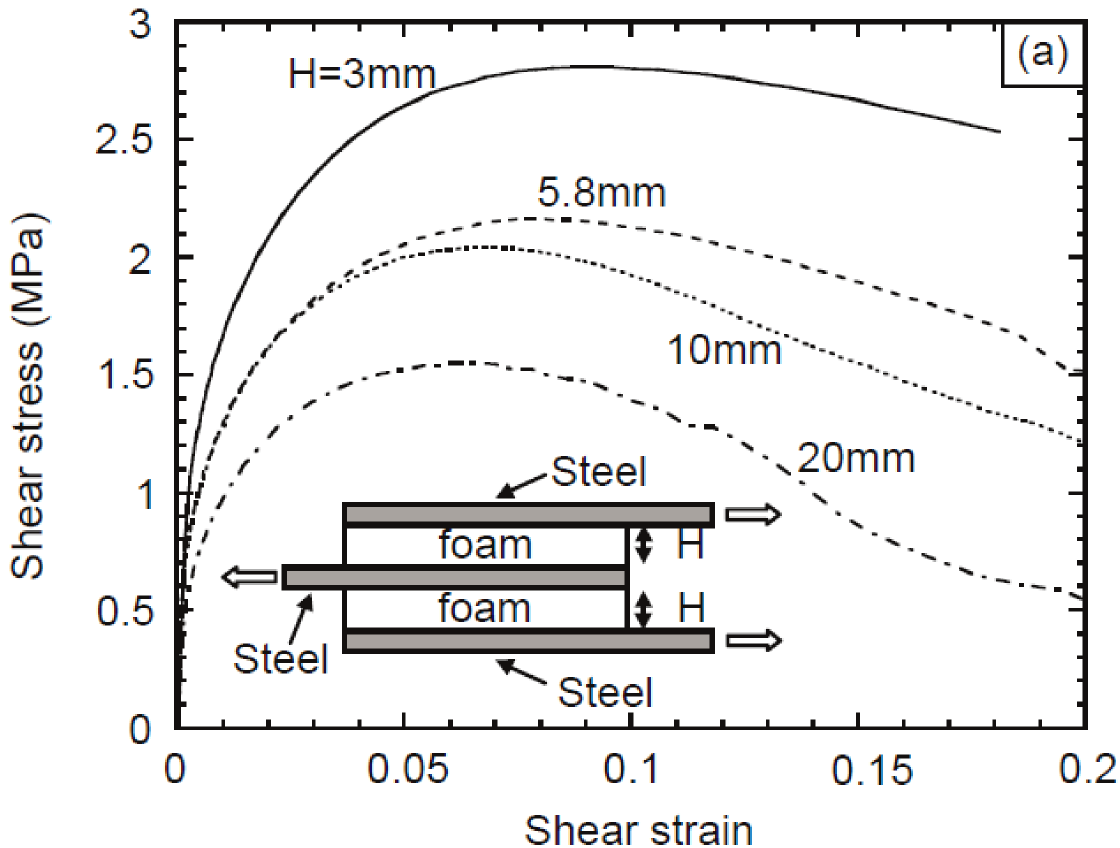

Effect of shear layer thickness in shear stress-strain response of Alporas foam (Experimental data from Chen & Fleck 2002)

Introduction

- Mechanical behavior of cellular materials (3)
  - Multi-scale behavior in nature
  - Intrinsic roles of different scale properties have to be accounted for
  - Macro-localization, micro-buckling, size effect phenomena have to be evaluated

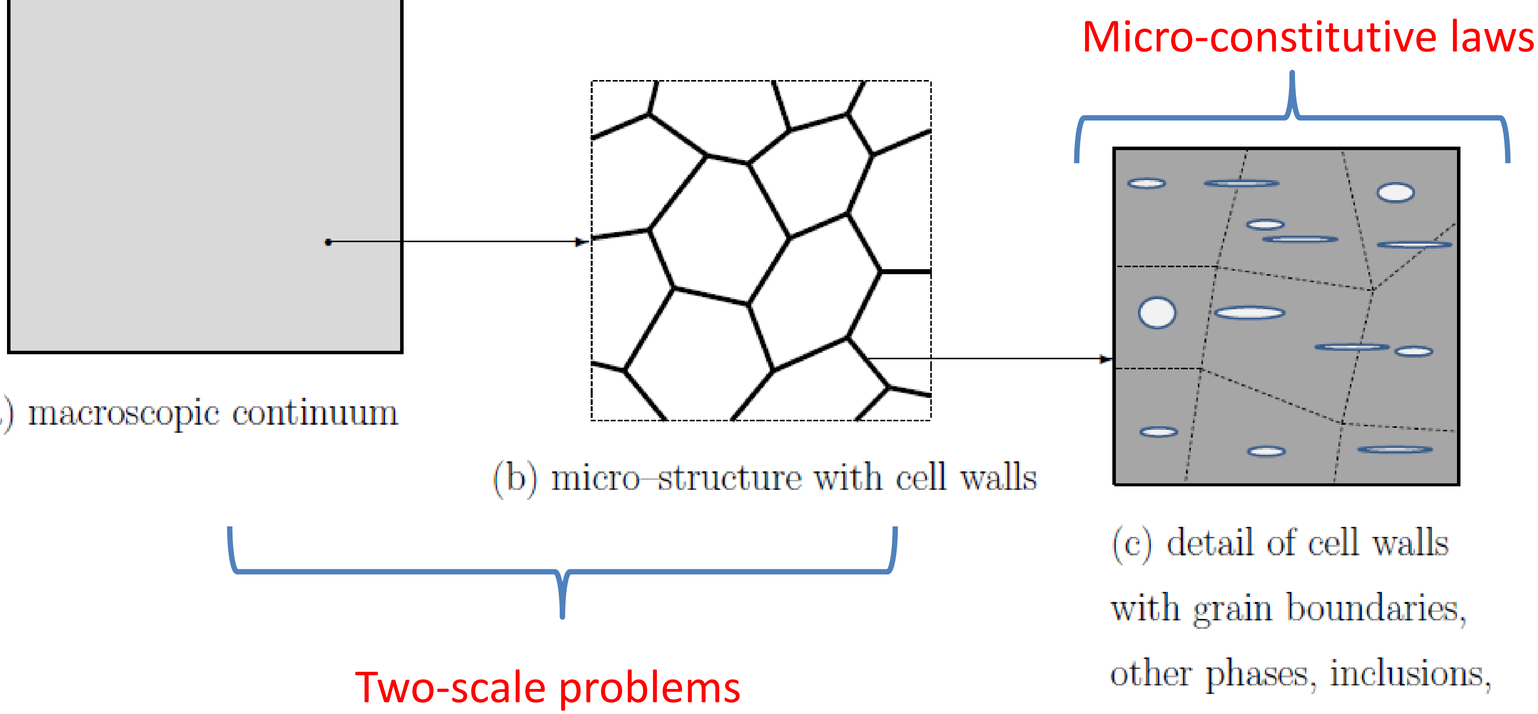

(a) macroscopic continuum

(b) micro–structure with cell walls

(c) detail of cell walls with grain boundaries, other phases, inclusions, voids, etc

- Finite element modeling strategies for cellular materials
  - Direct modeling-based approach
    - Direct models of cell struts, cell faces with beam, shell, bulk elements
  - Constitutive modeling-based approach
    - Cellular solids are considered as homogeneous media with suitable constitutive laws:
      - Phenomenological models
        - » Curve fitting, parameters identification from numerical or experimental results
      - Homogenization models
        - » Mean field, FFT, asymptotic, computational, etc.

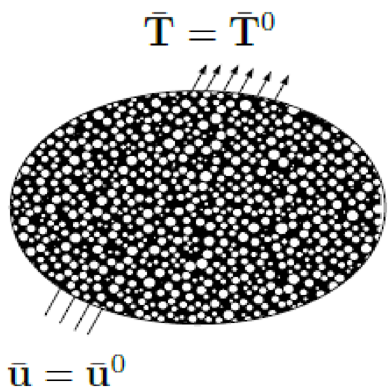

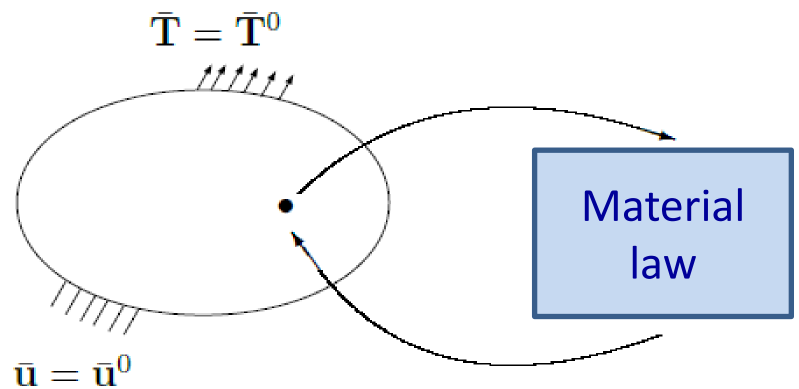

- Finite element modeling strategies for cellular materials (2)
  - Direct modeling-based approach
    - Advantages:
      - Capture directly localization due to micro-buckling & size effects
    - Drawbacks
      - Enormous number of DOFs
      - Difficult to construct the FE model due to geometry complexities
      - Suitable for small problems with limited dimensions

- Finite element modeling strategies for cellular materials (3)
  - Constitutive modeling-based approach
    - Advantages
      - Suitable for large problems
      - Micro-buckling, macro-localization & size effects can be captured with suitable constitutive models (e.g. computational homogenization)
    - Drawbacks
      - Phenomenological models
        - » Details of the micro-structure during macro-loading cannot be observed
        - » Material models and their parameters are difficult to be identified
      - Homogenization models
        - » Occurrence of micro-buckling phenomena is still limited in the mean - field, FFT, asymptotic homogenization frameworks

- Computational homogenization
  - This method is probably the most accurate method to directly account for complex micro-structural behaviors
  - This method can model:
    - Micro-buckling of cell walls (e.g. Okumura et al. 2004, Takahashi et al. 2010)
    - Localization problems (e.g. Kouznetsova et al. 2004, Massart et al. 2007, Nguyen et al. 2011, Coenen et al. 2012)
    - Size effects (e.g. Kouznetsova et al. 2004, Ebinger et al. (2005))

- First-order computational homogenization framework (first-order **FE²**)
  - Macro-scale
    - Finite element model
    - At one integration point $\bar{\mathbf{F}}$ is known, $\bar{\mathbf{P}}$ is sought
  - Micro-scale
    - Representative Volume Element (RVE)
    - Usual finite elements
    - Microscopic boundary conditions
  - Transition
    - Down-scaling: $\bar{\mathbf{F}}$ is used to define the BCs
    - Up-scaling: $\bar{\mathbf{P}}$ and $\partial\bar{\mathbf{P}}/\partial\bar{\mathbf{F}}$ are known from resolutions of micro-scale problems
  - Scale separation

$$l_{discrete} \ll l_{micro} \ll l_{macro}$$

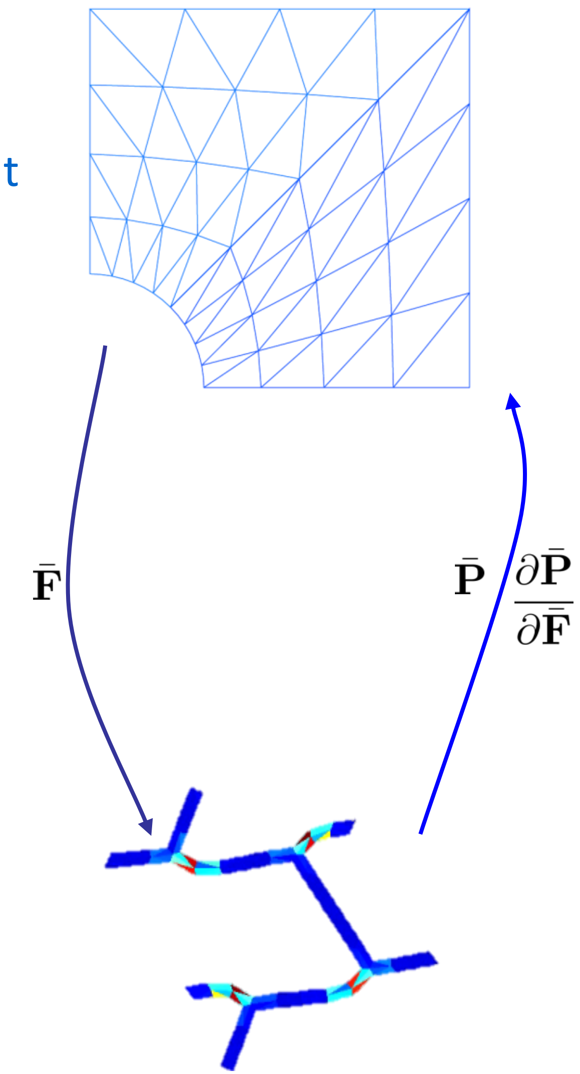

- Finite element solutions for strain softening problems suffer from:
  - Loss of solution uniqueness and strain localization
  - Mesh dependence

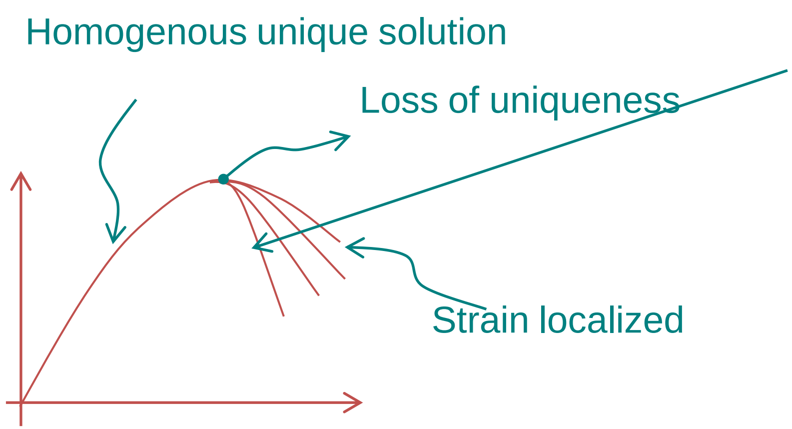

The numerical results change with the size of mesh and direction of mesh

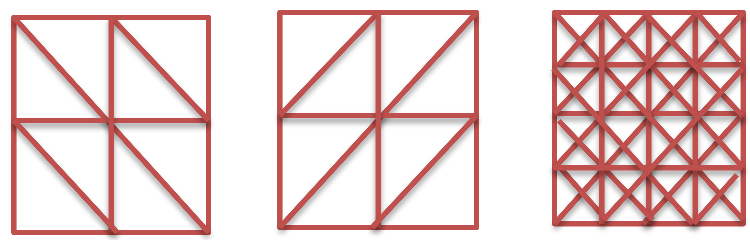

The numerical results change without convergence

- A generalized continuum is required at the macro-scale
  - Second-order computational homogenization framework (second-order **FE^2**) (Kouznetsova et al. 2004)
    - Macroscopic Mindlin strain gradient continuum
    - Microscopic classical continuum
    - Suitable for moderate localization bands & size effects

Introduction

- Second-order computational homogenization framework (second-order **FE²**)
  - Macro-scale
    - Mindlin strain gradient continuum

$$\bar{\mathbf{P}} \otimes \boldsymbol{\nabla}_0 - \bar{\mathbf{Q}} : (\boldsymbol{\nabla}_0 \otimes \boldsymbol{\nabla}_0) = \mathbf{0} \quad \text{in } B_0 \quad \& \quad \begin{cases} \bar{\mathbf{u}} = \bar{\mathbf{u}}^0 & \text{on } \partial_D B_0 \\ \bar{\mathbf{T}} = \bar{\mathbf{T}}^0 & \text{on } \partial_N B_0 \\ \mathrm{D}\bar{\mathbf{u}} = \mathrm{D}\bar{\mathbf{u}}^0 & \text{on } \partial_T B_0 \\ \bar{\mathbf{R}} = \bar{\mathbf{R}}^0 & \text{on } \partial_M B_0 \end{cases}$$

  - Micro-scale
    - Usual finite elements
    - Second-order microscopic boundary conditions
  - Transition
    - Down-scaling: $\bar{\mathbf{F}}, \bar{\mathbf{F}} \otimes \boldsymbol{\nabla}_0$ are used to define the BCs
    - Up-scaling: Two stresses $\bar{\mathbf{P}}, \bar{\mathbf{Q}}$ and
      4 tangent operators are known from resolutions of
      micro-scale problems

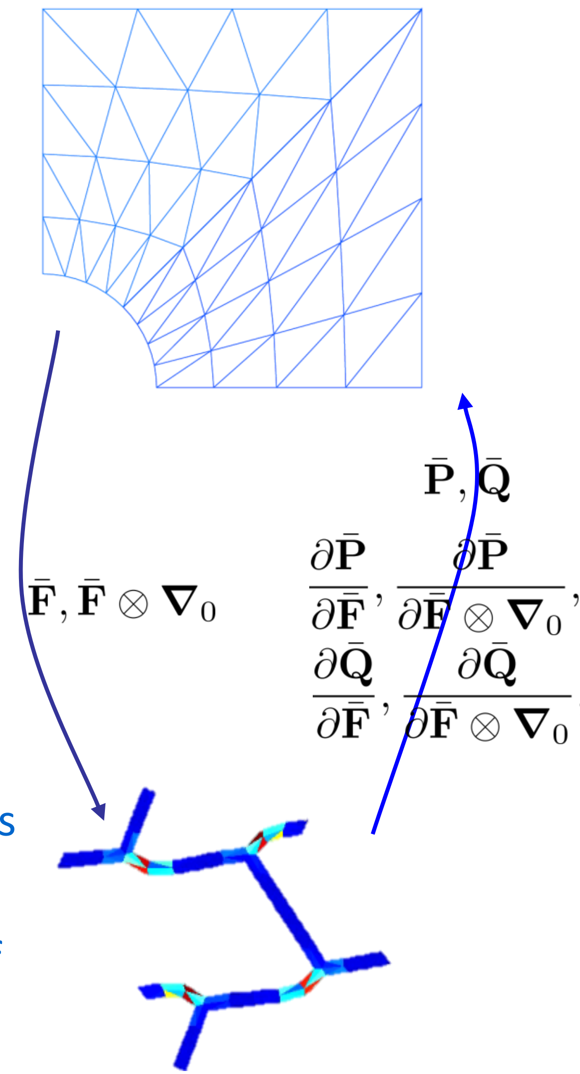

- Selected approach & challenges
  - Microscopic classical continuum with periodic boundary condition (PBC)

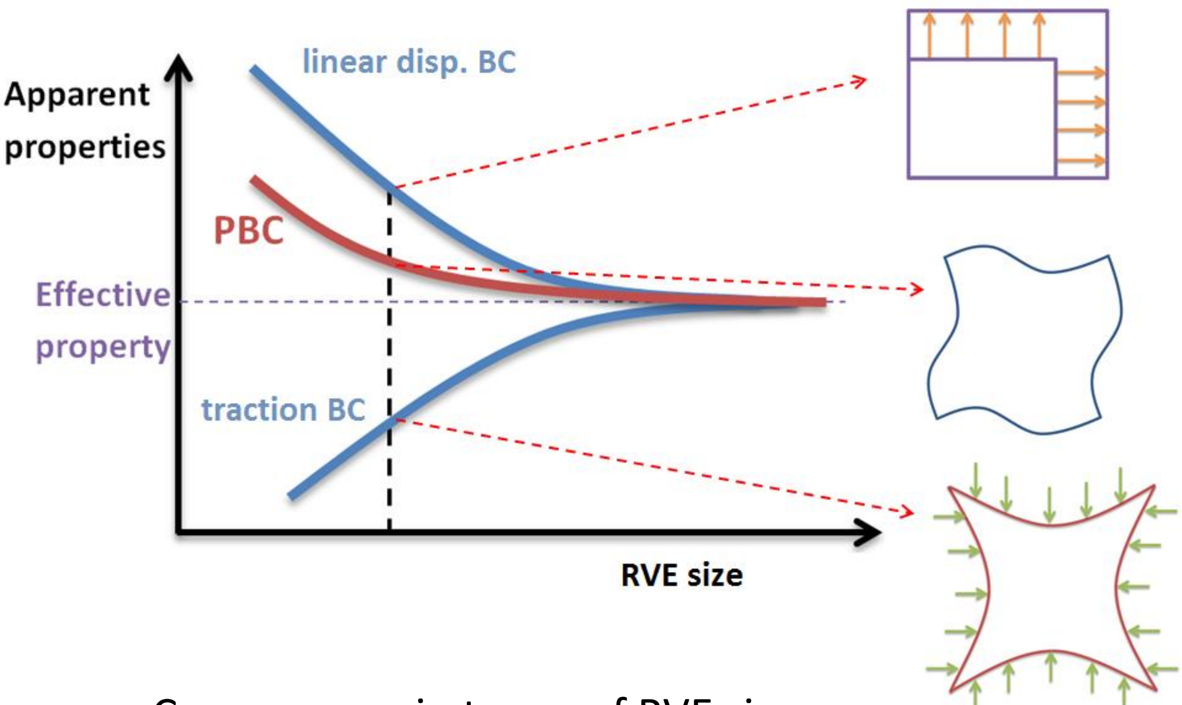

Convergence in terms of RVE size

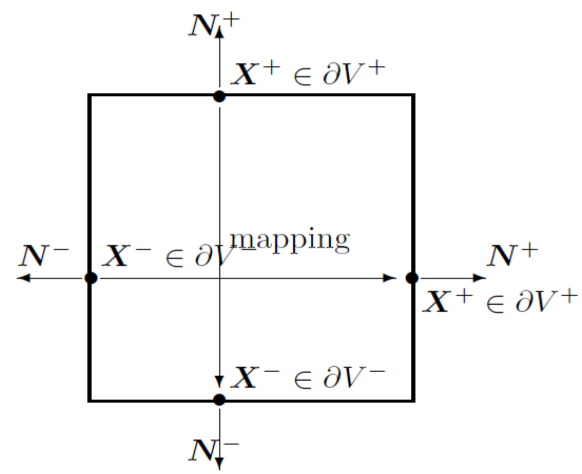

Matching nodes for PBC

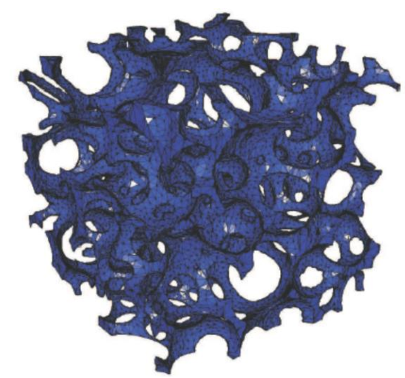

RVE example of random foam

→new method to enforce PBC on non-conforming meshes

- Selected approach & challenges (2)
  - Macroscopic Mindlin strain gradient continuum

$$\bar{\mathbf{P}} \otimes \boldsymbol{\nabla}_0 - \bar{\mathbf{Q}} : (\boldsymbol{\nabla}_0 \otimes \boldsymbol{\nabla}_0) = \mathbf{0} \quad \text{in } B_0 \quad \& \quad \begin{cases} \bar{\mathbf{u}} = \bar{\mathbf{u}}^0 & \text{on } \partial_D B_0 \\ \bar{\mathbf{T}} = \bar{\mathbf{T}}^0 & \text{on } \partial_N B_0 \\ \mathrm{D}\bar{\mathbf{u}} = \mathrm{D}\bar{\mathbf{u}}^0 & \text{on } \partial_T B_0 \\ \bar{\mathbf{R}} = \bar{\mathbf{R}}^0 & \text{on } \partial_M B_0 \end{cases}$$

→ efficient method to solve using usual finite elements

- Selected approach & challenges (3)
  - Instabilities at both scales

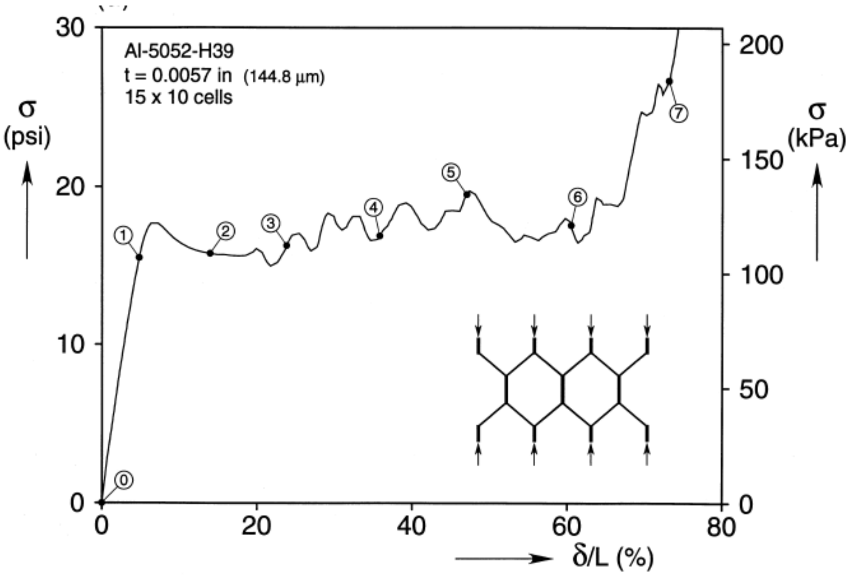

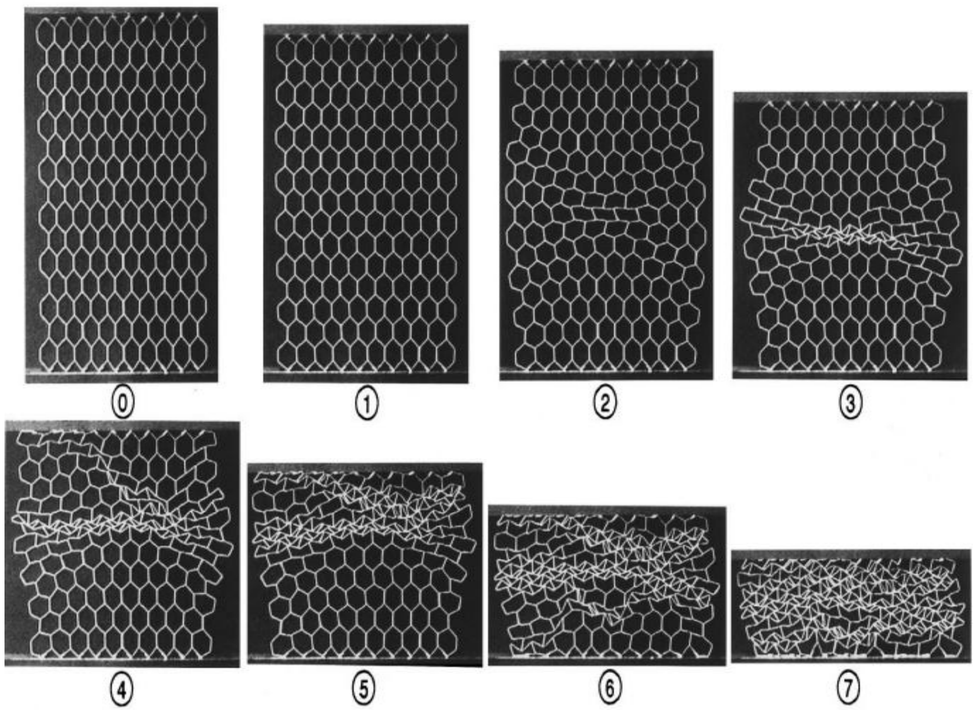

Force-displacement crushing response of aluminum honeycomb
(Experimental data from Papka & Kyriakides 1999)

→ arc-length method to capture instabilities

Topics

- PBC enforcement based on the ***polynomial interpolation method***

  (Nguyen, Geuzaine, Béchet & Noels CMS 2012)

- Second-order multi-scale computational homogenization scheme based on the Discontinuous Galerkin method (called ***second-order DG-based FE²* scheme**)
  - DG method is used to solved the macroscopic Mindlin strain gradient
  - Usual FE
  - Parallel computation

  (Nguyen, Becker & Noels CMAME 2013)

- Use of this ***second-order DG-based FE² scheme*** to capture instabilities in cellular materials
  - Arc-length path following method is adopted at both scales because of the presence of the macroscopic localization and micro-buckling
  - Parallel computation

  (Nguyen & Noels IJSS 2014)

- PBC enforcement based on the ***polynomial interpolation method***

(Nguyen, Geuzaine, Béchet & Noels CMS 2012)

- Second-order multi-scale computational homogenization scheme based on the Discontinuous Galerkin method (called ***second-order DG-based FE^2 scheme***)
  - DG method is used to solved the macroscopic Mindlin strain gradient
  - Usual FE
  - Parallel computation

(Nguyen, Becker & Noels CMAME 2013)

- Use of this ***second DG-based FE^2 scheme*** to capture instabilities in cellular materials
  - Arc-length path following method is adopted at both scales because of the presence of the macroscopic localization and micro-buckling
  - Parallel computation

(Nguyen & Noels IJSS 2014)

Polynomial interpolation method

- Periodic boundary condition
  - Defined from the fluctuation field
    - First-order: $\mathbf{w} = \mathbf{u} - (\bar{\mathbf{F}} - \mathbf{I}) \cdot \mathbf{X}$
    - Second-order:

$$\mathbf{w} = \mathbf{u} - (\bar{\mathbf{F}} - \mathbf{I}) \cdot \mathbf{X} - \frac{1}{2} (\bar{\mathbf{F}} \otimes \boldsymbol{\nabla}_0) : (\mathbf{X} \otimes \mathbf{X})$$

  - Stated on the RVE boundary
    - First-order PBC:

$$\mathbf{w}(\mathbf{X}^+) = \mathbf{w}(\mathbf{X}^-) \text{ and}$$
$$\mathbf{w}(\mathbf{X}^I) = \mathbf{0}$$

    - Second-order PBC:

$$\mathbf{w}(\mathbf{X}^+) = \mathbf{w}(\mathbf{X}^-) \text{ and}$$
$$\int_{S_i} \mathbf{w}(\mathbf{X})\, d\partial V = \mathbf{0} \quad \forall S_i \subset \partial V_0$$

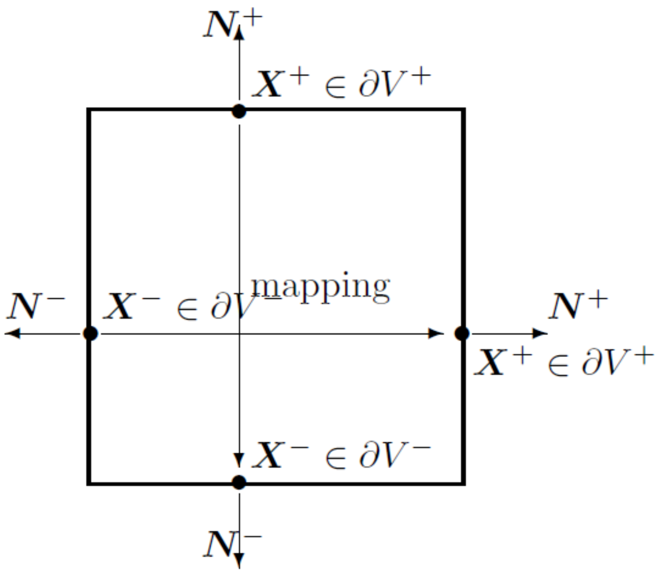

  - Can be achieved by constraining opposite nodes

- Cellular materials
  - Usually random meshes
  - Important voids on the boundaries

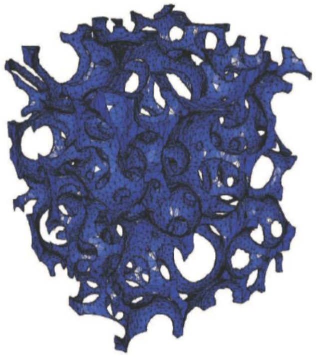

- Enforcement of the periodic boundary condition in FEM
  - For conforming meshes
    - Directly constrains on matching nodes

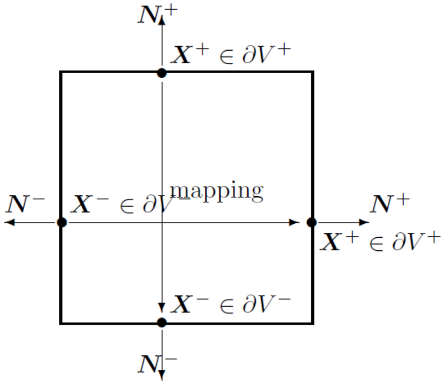

  - For general meshes
    - Slave/master approach (Yuan et al. 2008)
    - Weak periodicity (Larson et al. 2011)
    - Local implementation (Tyrus et al. 2008)

No void part on the RVE boundary

  - Polynomial interpolation method (Nguyen et al. 2012)
    - For arbitrary RVE geometries

- Polynomial interpolation method for PBC enforcement

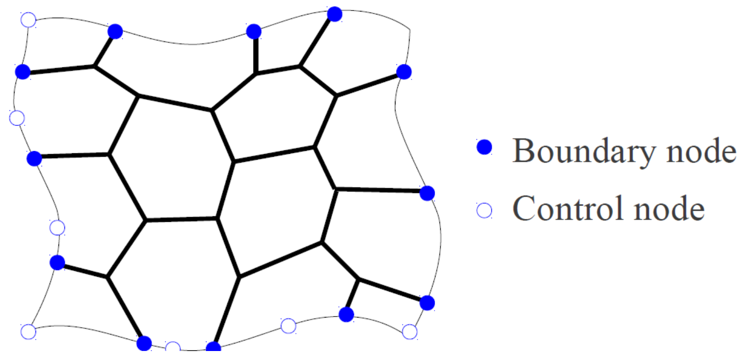

  – Use of control nodes (new or existing nodes) to interpolate the fluctuation field at the RVE boundary

  – Use of interpolant functions (e.g. Lagrange, cubic spline , patch Coons, etc.)

  – Fluctuations at boundary nodes are interpolated from control nodes

  – PBC is satisfied by using the same interpolation form for opposite parts

- Polynomial interpolation method for PBC enforcement (2)
  - First-order PBC

$$\mathbf{w}^{-}(\mathbf{X}) = \sum_k \mathbb{N}^k(\mathbf{X})\,\mathbf{w}^k + \sum_k \mathbb{M}^k(\mathbf{X})\,\boldsymbol{\theta}^k\,,$$

$$\mathbf{w}^{+}(\mathbf{X}) = \sum_k \mathbb{N}^k(\mathbf{X})\,\mathbf{w}^k + \sum_k \mathbb{M}^k(\mathbf{X})\,\boldsymbol{\theta}^k \text{ and}$$

$$\mathbf{w}\left(\mathbf{X}^I\right) = \mathbf{0}$$

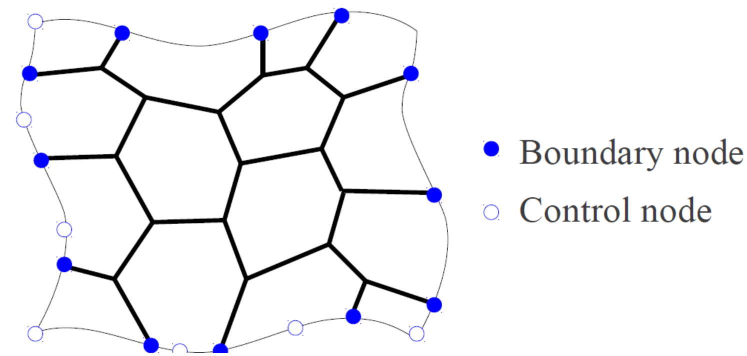

  - Second-order PBC

$$\mathbf{w}^{-}(\mathbf{X}) = \sum_k \mathbb{N}^k(\mathbf{X})\,\mathbf{w}^k + \sum_k \mathbb{M}^k(\mathbf{X})\,\boldsymbol{\theta}^k\,,$$

$$\mathbf{w}^{+}(\mathbf{X}) = \sum_k \mathbb{N}^k(\mathbf{X})\,\mathbf{w}^k + \sum_k \mathbb{M}^k(\mathbf{X})\,\boldsymbol{\theta}^k \text{ and}$$

$$\int_{S\subset\partial V^-}\left(\sum_k \mathbb{N}^k(\mathbf{X})\,\mathbf{w}^k + \sum_k \mathbb{M}^k(\mathbf{X})\,\boldsymbol{\theta}^k\right) d\partial V = \mathbf{0}$$

  - Interpolant functions $\mathbb{N}^k, \mathbb{M}^k$ and control DOFs $\mathbf{w}^k, \boldsymbol{\theta}^k$ depend on the interpolation methods

- Polynomial interpolation method for PBC enforcement (3)
  - Results in new constraints in terms of displacements of both boundary and control nodes $\tilde{\mathbf{C}}\tilde{\mathbf{u}}_b - \mathbf{g} = \mathbf{0}$
    - First order: $\mathbf{g} = \mathbf{g}\left(\bar{\mathbf{F}}\right)$
    - Second-order: $\mathbf{g} = \mathbf{g}\left(\bar{\mathbf{F}}, \bar{\mathbf{F}} \otimes \boldsymbol{\nabla}_0\right)$
  - These linear constraints can be enforced by
    - Constraints elimination
    - Lagrange multipliers
  - Suitable for
    - Arbitrary meshes
    - Important void parts on the RVE boundaries
    - Arbitrary interpolation forms

Polynomial interpolation method

- 2D problems using Lagrange & cubic spline interpolations
  - Periodic hole structures
    - Hole radius = 0.2 mm
    - Elastic material: Young modulus= 70 GPa, Poisson ratio = 0.3

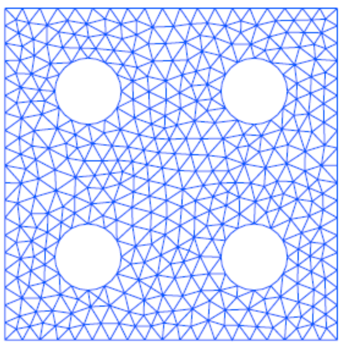

Periodic mesh

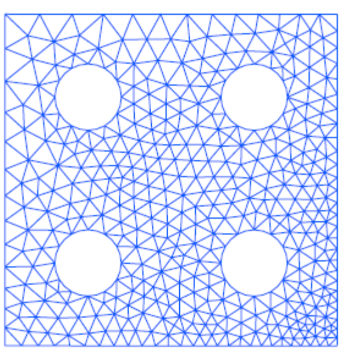

Non-periodic mesh

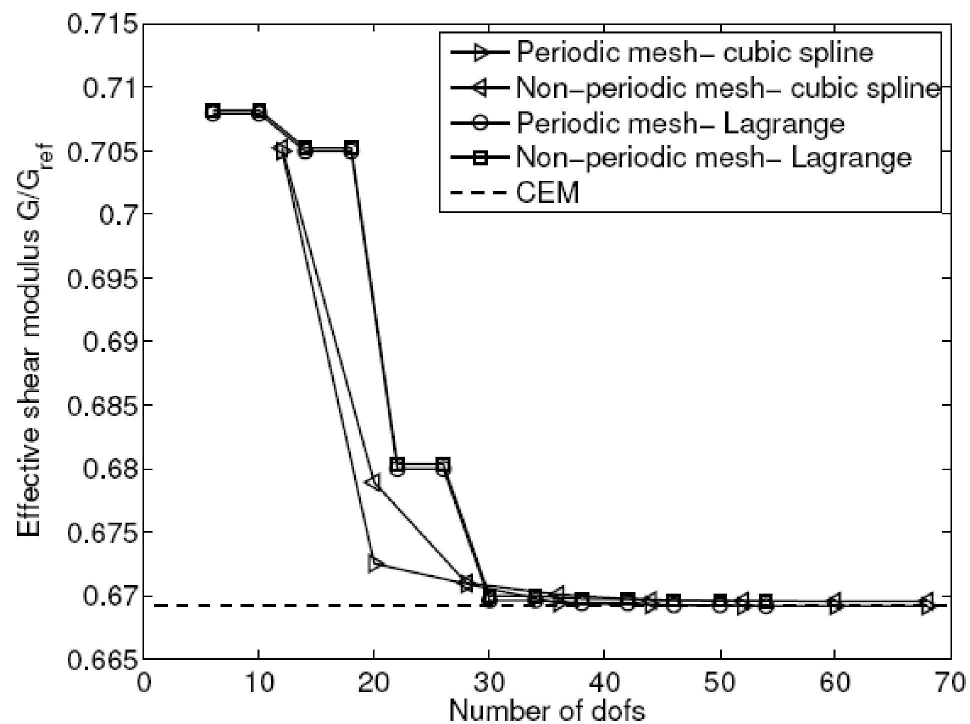

Convergence of effective properties in terms of new DOFs added to system

CEM: method based on matching nodes

- 2D problems using Lagrange & cubic spline interpolations (2)
  - Honeycomb structures
    - Edge length = 1 mm & thickness = 0.1 mm
    - Elastic material: Young modulus= 68.9 GPa, Poisson ratio = 0.33

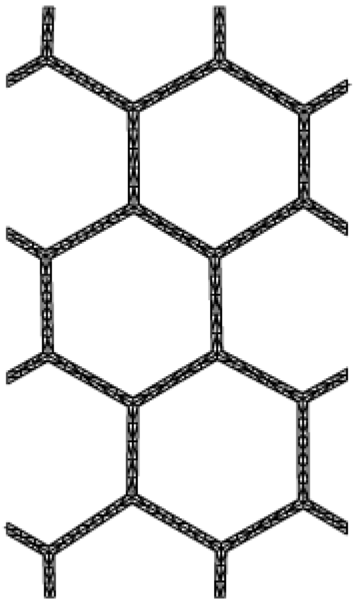

RVE mesh from honeycomb structure

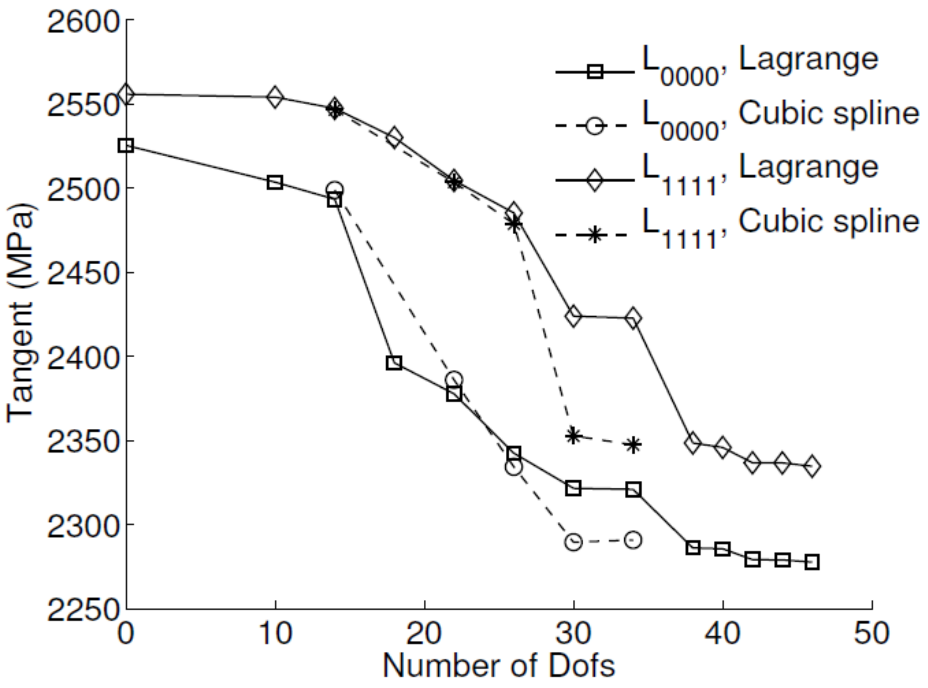

Convergence of effective properties in terms of new DOFs added to system

Polynomial interpolation method

- 3D problems using the patch Coons interpolation based on the Lagrange & cubic spline interpolations

$$\bar{\varepsilon} = \begin{bmatrix} 0.01 & 0.005 & 0.005 \\ 0.005 & 0.01 & -0.005 \\ 0.005 & -0.005 & -0.01 \end{bmatrix}$$

$$\bar{\sigma}_{\text{Lagrange}} = \begin{bmatrix} 281.583 & 92.392 & 121.181 \\ 92.392 & 270.111 & -115.835 \\ 121.181 & -115.835 & -247.78 \end{bmatrix} \text{MPa}$$

$$\bar{\sigma}_{\text{spline}} = \begin{bmatrix} 281.399 & 91.9833 & 121.239 \\ 91.983 & 268.85 & -115.614 \\ 121.239 & -115.614 & -248.214 \end{bmatrix} \text{MPa}$$

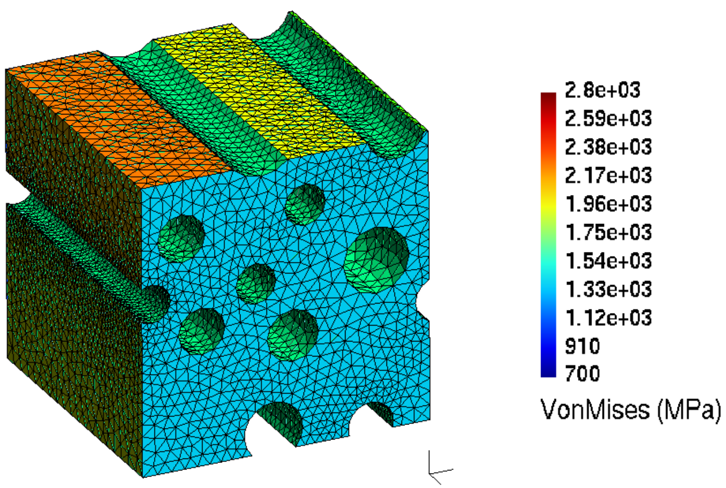

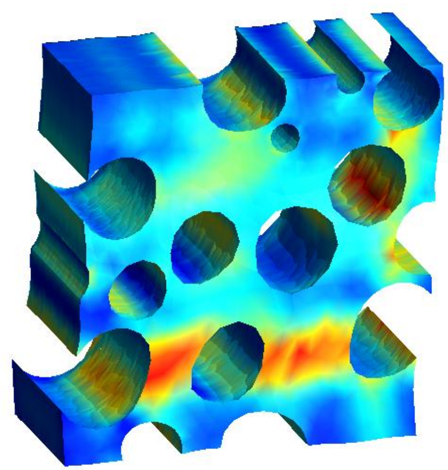

Lagrange Coons patch of order 15

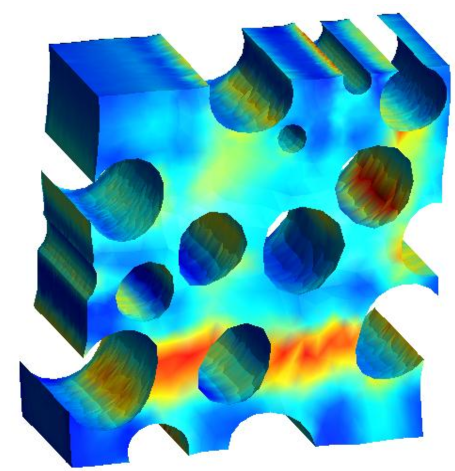

Cubic spline Coons patch with 10 segments

- Conclusions
  - A new method to enforce the PBC is presented
    - By using an interpolation formulation
    - For arbitrary meshes
    - For both 2-dimensional and 3-dimensional problems
  - This method provides a better estimation compared to the linear displacement BC which is usually used for non-conforming meshes
  - The key advantage of this method is the elimination of the need of matching nodes

- PBC enforcement based on the ***polynomial interpolation method***

  (Nguyen, Geuzaine, Béchet & Noels CMS 2012)

- Second-order multi-scale computational homogenization scheme based on the Discontinuous Galerkin method (called ***second-order DG-based FE^2 scheme***)
  – DG method is used to solved the macroscopic Mindlin strain gradient
  – Usual FE
  – Parallel computation

  (Nguyen, Becker & Noels CMAME 2013)

- Use of this second DG-based FE2 scheme to capture instabilities in cellular materials
  – Arc-length path following method is adopted at both scales because of the presence of the macroscopic localization and micro-buckling
  – Parallel computation

  (Nguyen & Noels IJSS 2014)

- Mindlin strain gradient

$$\bar{\mathbf{P}} \otimes \boldsymbol{\nabla}_0 - \bar{\mathbf{Q}} : (\boldsymbol{\nabla}_0 \otimes \boldsymbol{\nabla}_0) = \mathbf{0} \quad \text{in } B_0 \quad \& \quad \begin{cases} \bar{\mathbf{u}} = \bar{\mathbf{u}}^0 & \text{on } \partial_D B_0 \\ \bar{\mathbf{T}} = \bar{\mathbf{T}}^0 & \text{on } \partial_N B_0 \\ \mathrm{D}\bar{\mathbf{u}} = \mathrm{D}\bar{\mathbf{u}}^0 & \text{on } \partial_T B_0 \\ \bar{\mathbf{R}} = \bar{\mathbf{R}}^0 & \text{on } \partial_M B_0 \end{cases}$$

- Numerical solution requires the continuity of the displacement field and of its derivatives. Some methods can be considered:
  - Mixed methods (*e.g.* Shu et al. 1999)
  - Mesh-less method (*e.g.* Askes et al. 2002)
  - ***C***^{1} finite elements (*e.g.* Papanicolopulos et al. 2012)
  - Discontinuous Galerkin (DG) method (*e.g.* Engel et al. 2002)

- DG method is extended to large deformations and multi-scale analyses to solve the Mindlin strain gradient continuum
  - Using only the displacement field as unknowns
  - Enforcing weakly inter-element continuities

- Finite element discretization
- Same **discontinuous** polynomial approximation for
  - Test function φ_h
  - Trial function $\delta\varphi$

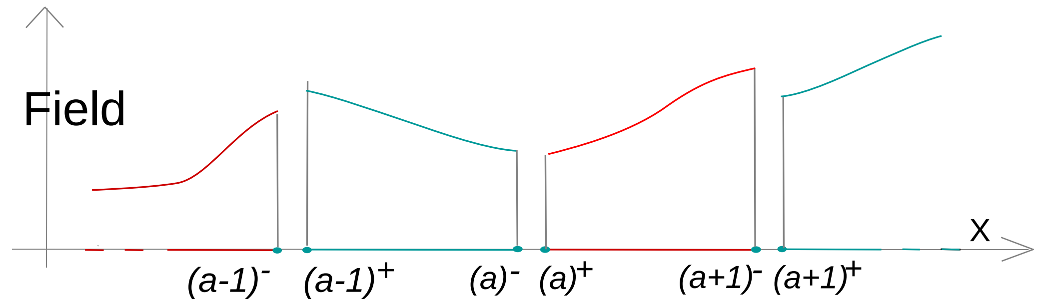

- Definition of trace operators on the inter-element interfaces
  - Jump operator $[\![\bullet]\!] = \bullet^+ - \bullet^-$
  - Mean operator $\langle\bullet\rangle = \frac{1}{2}\left(\bullet^+ + \bullet^-\right)$
- Continuity is weakly enforced, such that the method
  - Is consistent
  - Is stable
  - Has an optimal convergence rate

- As the strain gradient solution requires the C^0 & C^1 continuities, two formulations can be used:
  - Full Discontinuous Galerkin (FDG) formulation

$$\begin{cases}\mathbf{U}^k = \left\{\bar{\mathbf{u}} \in \mathbf{L}^2\left(B_0\right) \quad \middle| \quad \bar{\mathbf{u}}|_{\Omega_0^e} \in \mathbb{P}^k \forall \Omega_e^0 \in B_0\right\} \\ \mathbf{U}_c^k = \left\{\delta\bar{\mathbf{u}} \in \mathbf{U}^k \quad \middle| \quad \delta\bar{\mathbf{u}}|_{\partial_D B_0} = \mathbf{0}\right\}\end{cases}$$

- Weak enforcement of C^0 & C^1 continuities
- Different DOFs at inter-element interfaces
- Usual shape functions

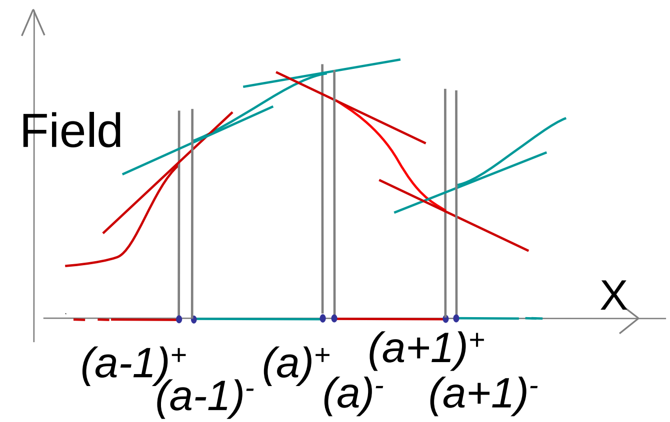

  - Enriched Discontinuous Galerkin (EDG) formulation

$$\begin{cases}\mathbf{U}^k = \left\{\bar{\mathbf{u}} \in \mathbf{H}^1\left(B_0\right) \quad \middle| \quad \bar{\mathbf{u}}|_{\Omega_0^e} \in \mathbb{P}^k \quad \forall \Omega_e^0 \in B_0\right\} \\ \mathbf{U}_c^k = \left\{\delta\bar{\mathbf{u}} \in \mathbf{U}^k \quad \middle| \quad \delta\bar{\mathbf{u}}|_{\partial_D B_0} = \mathbf{0}\right\}\end{cases}$$

- Weak enforcement of C^1 continuity
- Same DOFs as conventional FEM
- Usual shape functions

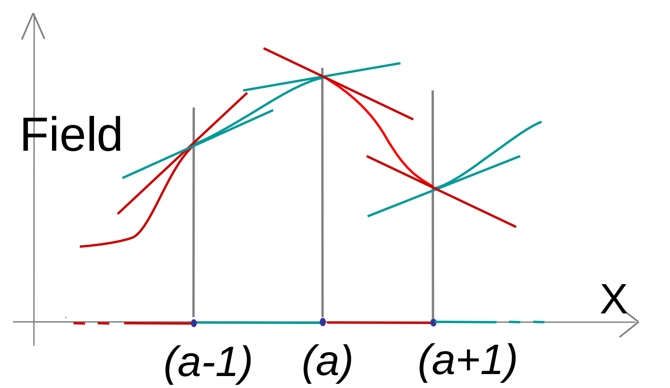

DG method for strain gradient problems

- Weak formulation obtained by repeating integrations by parts on each element :

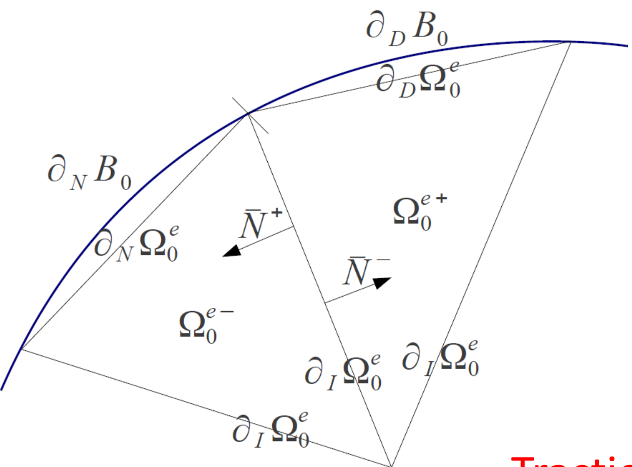

$$\sum_e \int_{\Omega_0^e} \delta\bar{\mathbf{u}} \cdot \left[\bar{\mathbf{P}} \otimes \boldsymbol{\nabla}_0 - \bar{\mathbf{Q}} : (\boldsymbol{\nabla}_0 \otimes \boldsymbol{\nabla}_0)\right] dB = 0$$

$$\int_{\partial B_0} \delta\bar{\mathbf{u}} \cdot \bar{\hat{\mathbf{P}}} \cdot \bar{\mathbf{N}} + (\delta\bar{\mathbf{u}} \otimes \boldsymbol{\nabla}_0) : \left(\bar{\mathbf{Q}} \cdot \bar{\mathbf{N}}\right) d\partial B$$
$$+ \sum_e \int_{\partial_I \Omega_0^e} \delta\bar{\mathbf{u}} \cdot \bar{\hat{\mathbf{P}}} \cdot \bar{\mathbf{N}} + (\delta\bar{\mathbf{u}} \otimes \boldsymbol{\nabla}_0) : \bar{\mathbf{Q}} \cdot \bar{\mathbf{N}}\, d\partial B$$
$$- \int_{B_0} \left[\bar{\mathbf{P}} : (\delta\bar{\mathbf{u}} \otimes \boldsymbol{\nabla}_0) + \bar{\mathbf{Q}} \vdots (\delta\bar{\mathbf{u}} \otimes \boldsymbol{\nabla}_0 \otimes \boldsymbol{\nabla}_0)\right] dB = 0$$

Traction BC

Second-order interface term

$$\int_{\partial B_0} \delta\bar{\mathbf{u}} \cdot \bar{\hat{\mathbf{P}}} \cdot \bar{\mathbf{N}} + (\delta\bar{\mathbf{u}} \otimes \boldsymbol{\nabla}_0) : \left(\bar{\mathbf{Q}} \cdot \bar{\mathbf{N}}\right) d\partial B$$

$$- \int_{\partial_I B_0} [\![\delta\bar{\mathbf{u}} \cdot \bar{\hat{\mathbf{P}}}]\!] \cdot \bar{\mathbf{N}}\, d\partial B \quad - \int_{\partial_I B_0} [\![(\delta\bar{\mathbf{u}} \otimes \boldsymbol{\nabla}_0) : \bar{\mathbf{Q}}]\!] \cdot \bar{\mathbf{N}}\, d\partial B$$

$$- \int_{B_0} \left[\bar{\mathbf{P}} : (\delta\bar{\mathbf{u}} \otimes \boldsymbol{\nabla}_0) + \bar{\mathbf{Q}} \vdots (\delta\bar{\mathbf{u}} \otimes \boldsymbol{\nabla}_0 \otimes \boldsymbol{\nabla}_0)\right] dB = 0$$

First-order interface term

$$\bar{\hat{\mathbf{P}}} = \bar{\mathbf{P}} - \bar{\mathbf{Q}} \cdot \boldsymbol{\nabla}_0$$

Bulk term

- First-order interface term

$$\int_{\partial_I B_0} \left[\!\left[\delta\bar{\mathbf{u}}\cdot\hat{\bar{\mathbf{P}}}\right]\!\right]\cdot\bar{\mathbf{N}}\,d\partial B$$

is rewritten as the sum of three terms:

  - Consistency

$$\int_{\partial_I B_0} [\![\delta\bar{\mathbf{u}}]\!]\cdot\left\langle\hat{\bar{\mathbf{P}}}\right\rangle\cdot\bar{\mathbf{N}}^-\,d\partial B$$

  - Compatibility

$$\int_{\partial_I B_0} [\![\bar{\mathbf{u}}]\!]\cdot\left\langle\hat{\bar{\mathbf{P}}}\left(\delta\bar{\mathbf{u}}\right)\right\rangle\cdot\bar{\mathbf{N}}^-\,d\partial B$$

  - Stability controlled by β_P

$$\int_{\partial_I B_0}\left([\![\bar{\mathbf{u}}]\!]\otimes\bar{\mathbf{N}}^-\right):\left\langle\frac{\beta_P}{h_s}\mathbb{C}^0\right\rangle:\left(\delta\bar{\mathbf{u}}\otimes\bar{\mathbf{N}}^-\right)\,d\partial B$$

  - These terms vanish in the case of EDG formulation

- Second-order interface term

$$\int_{\partial_I B_0}\left[\!\left[(\delta\bar{\mathbf{u}}\otimes\boldsymbol{\nabla}_0):\bar{\mathbf{Q}}\right]\!\right]\cdot\bar{\mathbf{N}}\,d\partial B$$

is rewritten as the sum of three terms:

  - Consistency

$$\int_{\partial_I B_0}[\![\delta\bar{\mathbf{u}}\otimes\boldsymbol{\nabla}_0]\!]:\langle\bar{\mathbf{Q}}\rangle\cdot\bar{\mathbf{N}}^-\,d\partial B$$

  - Compatibility

$$\int_{\partial_I B_0}[\![\bar{\mathbf{u}}\otimes\boldsymbol{\nabla}_0]\!]:\langle\bar{\mathbf{Q}}\left(\delta\bar{\mathbf{u}}\right)\rangle\cdot\bar{\mathbf{N}}^-\,d\partial B$$

  - Stability controlled by β_Q

$$\int_{\partial_I B_0}\left([\![\bar{\mathbf{u}}\otimes\boldsymbol{\nabla}_0]\!]\otimes\bar{\mathbf{N}}^-\right)\,\vdots\,\left\langle\frac{\beta_Q}{h_s}\mathbb{J}^0\right\rangle\,\vdots\,\left([\![\delta\bar{\mathbf{u}}\otimes\boldsymbol{\nabla}_0]\!]\otimes\bar{\mathbf{N}}^-\right)\,d\partial B$$

h_s characteristic mesh size

DG method for strain gradient problems

- Weak formulation obtained by DG method: $\mathrm{a}(\bar{\mathbf{u}}, \delta\bar{\mathbf{u}}) = \mathrm{b}(\delta\bar{\mathbf{u}}) \qquad \forall \delta\bar{\mathbf{u}} \in \mathbf{U}_c^k$
- Bi-nonlinear term: $\mathrm{a}(\bar{\mathbf{u}}, \delta\bar{\mathbf{u}}) = \mathrm{a}^{\mathrm{bulk}}(\bar{\mathbf{u}}, \delta\bar{\mathbf{u}}) + \mathrm{a}^{\mathrm{PI}}(\bar{\mathbf{u}}, \delta\bar{\mathbf{u}}) + \mathrm{a}^{\mathrm{QI}}(\bar{\mathbf{u}}, \delta\bar{\mathbf{u}})$
  - Bulk term

$$\mathrm{a}^{\mathrm{bulk}}(\bar{\mathbf{u}}, \delta\bar{\mathbf{u}}) = \int_{B_0} \left[\bar{\mathbf{P}} : (\delta\bar{\mathbf{u}} \otimes \boldsymbol{\nabla}_0) + \bar{\mathbf{Q}} \,\vdots\, (\delta\bar{\mathbf{u}} \otimes \boldsymbol{\nabla}_0 \otimes \boldsymbol{\nabla}_0)\right] dB$$

  - First-order interface term (vanishes if using the EDG formulation)

$$\begin{aligned}\mathrm{a}^{\mathrm{PI}}(\bar{\mathbf{u}}, \delta\bar{\mathbf{u}}) = & \int_{\partial_I B_0} \Big[[\![\delta\bar{\mathbf{u}}]\!] \cdot \left\langle \hat{\bar{\mathbf{P}}}(\bar{\mathbf{u}}) \right\rangle \cdot \bar{\mathbf{N}}^- + [\![\bar{\mathbf{u}}]\!] \cdot \left\langle \hat{\bar{\mathbf{P}}}(\delta\bar{\mathbf{u}}) \right\rangle \cdot \bar{\mathbf{N}}^- \\ & + [\![\bar{\mathbf{u}}]\!] \otimes \bar{\mathbf{N}}^- : \left\langle \frac{\beta_P}{h_s} \mathbf{C}^0 \right\rangle : [\![\delta\bar{\mathbf{u}}]\!] \otimes \bar{\mathbf{N}}^- \Big] \, d\partial B ,\end{aligned}$$

  - Second-order interface term

$$\begin{aligned}\mathrm{a}^{\mathrm{QI}}(\bar{\mathbf{u}}, \delta\bar{\mathbf{u}}) = & \int_{\partial_I B_0} \Big[[\![\delta\bar{\mathbf{u}} \otimes \boldsymbol{\nabla}_0]\!] : \left\langle \bar{\mathbf{Q}}(\bar{\mathbf{u}}) \right\rangle \cdot \bar{\mathbf{N}}^- + [\![\bar{\mathbf{u}} \otimes \boldsymbol{\nabla}_0]\!] : \left\langle \bar{\mathbf{Q}}(\delta\bar{\mathbf{u}}) \right\rangle \cdot \bar{\mathbf{N}}^- \\ & + [\![\bar{\mathbf{u}} \otimes \boldsymbol{\nabla}_0]\!] \otimes \bar{\mathbf{N}}^- \,\vdots\, \left\langle \frac{\beta_Q}{h_s} \mathbf{J}^0 \right\rangle \,\vdots\, [\![\delta\bar{\mathbf{u}} \otimes \boldsymbol{\nabla}_0]\!] \otimes \bar{\mathbf{N}}^- \Big] \, d\partial B .\end{aligned}$$

- Load term

$$\mathrm{b}(\delta\bar{\mathbf{u}}) = \left(\int_{\partial_N B_0} \bar{\mathbf{T}}^0 \cdot \delta\bar{\mathbf{u}} \, d\partial B + \int_{\partial_M B_0} \bar{\mathbf{R}}^0 \cdot \mathrm{D}\delta\bar{\mathbf{u}} \, d\partial B \right)$$

DG method for strain gradient problems

- Second-order DG-based FE² scheme
  - DG solution of macroscopic Mindlin strain gradient problems
    - Interface & bulk integration points
  - Microscopic problems
    - Associated with both interface & bulk integration points
  - Scale transitions
    - Down-scaling: two kinematic strains are used to define the microscopic BCs
    - Up-scaling: two stresses and 4 tangent operators are extracted from the resolutions of the microscopic problems

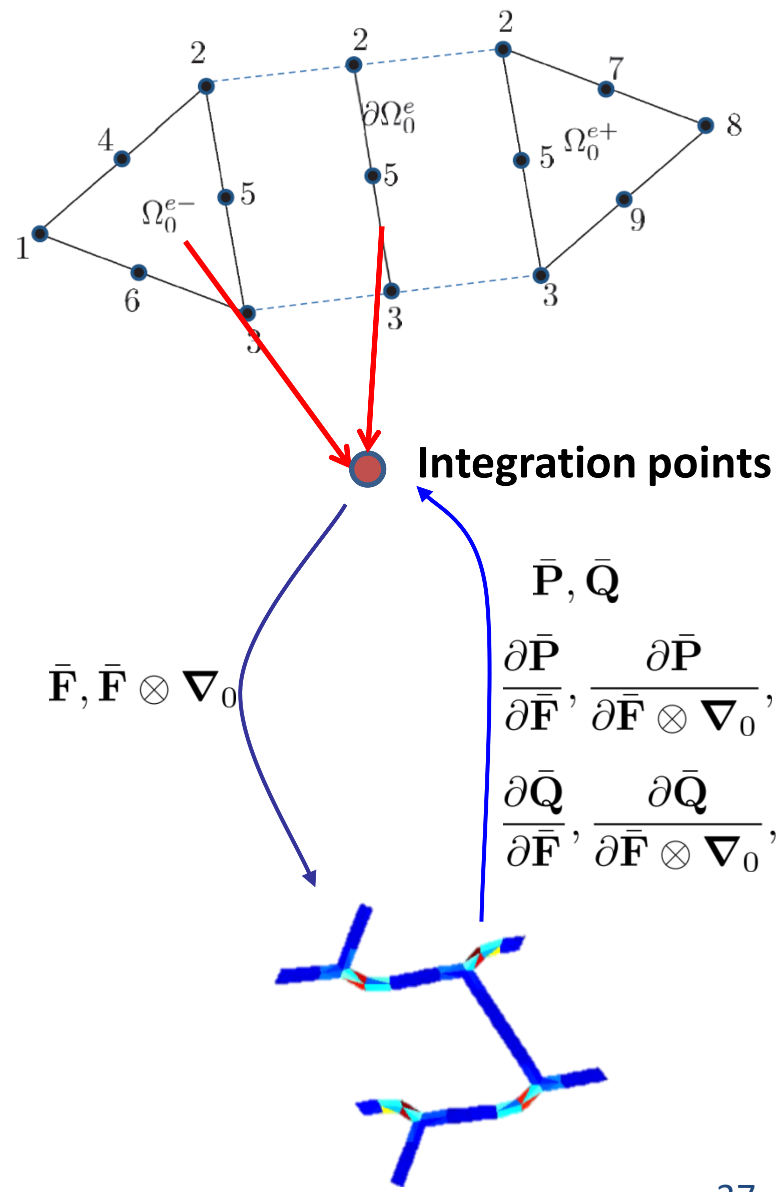

- Parallel second-order DG-based FE^2 scheme
  - Computation strategy

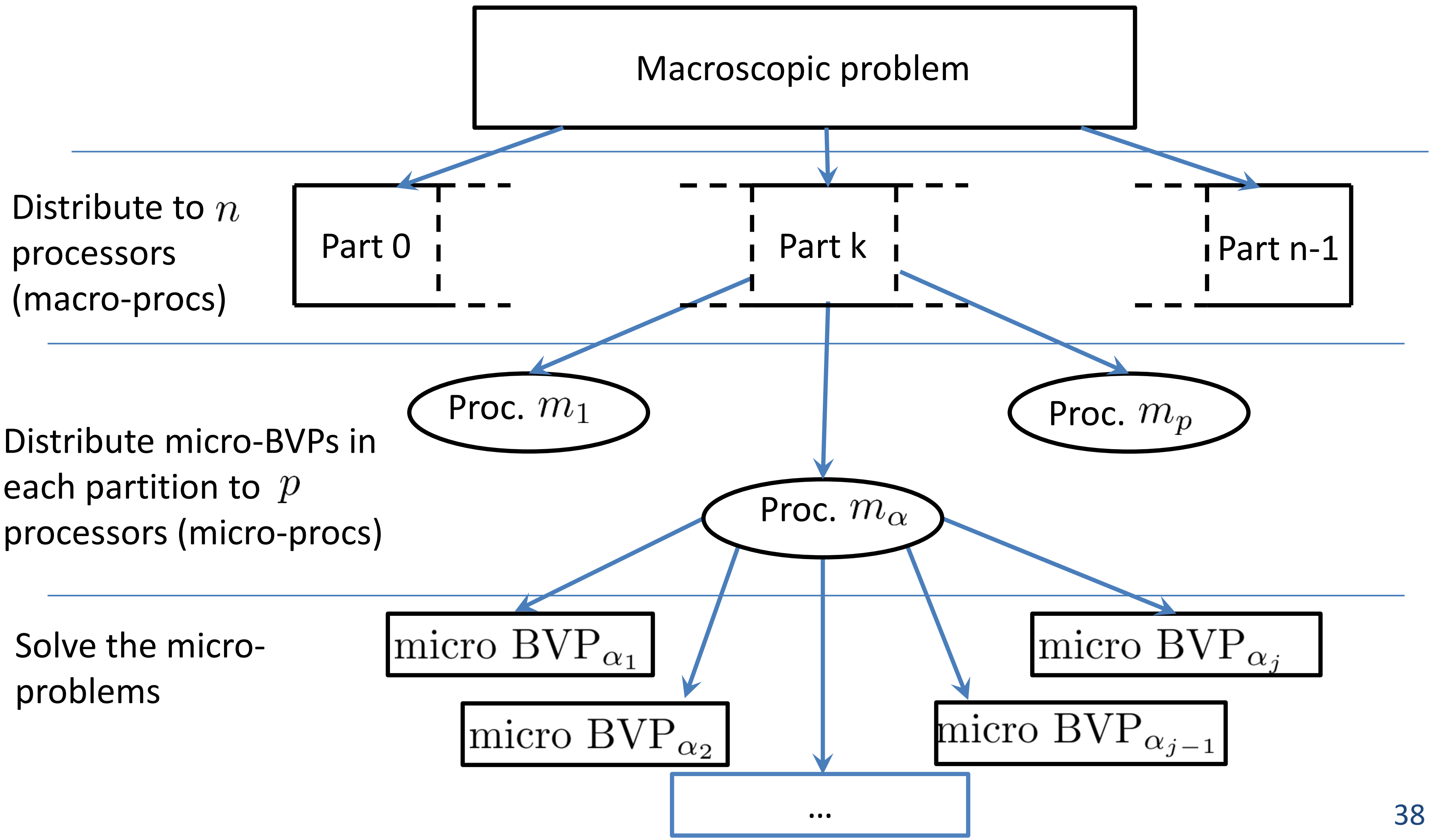

- Parallel second-order DG-based FE^2 scheme (2)
  - At the macro-scale
    - Macro-scale parallelization
    - Computation using FDG formulation with "ghost elements"
      - Communications required at each time step to exchange the nodal displacements at inter-partition interfaces only
  - At the micro-scale
    - All microscopic problems are separate in nature

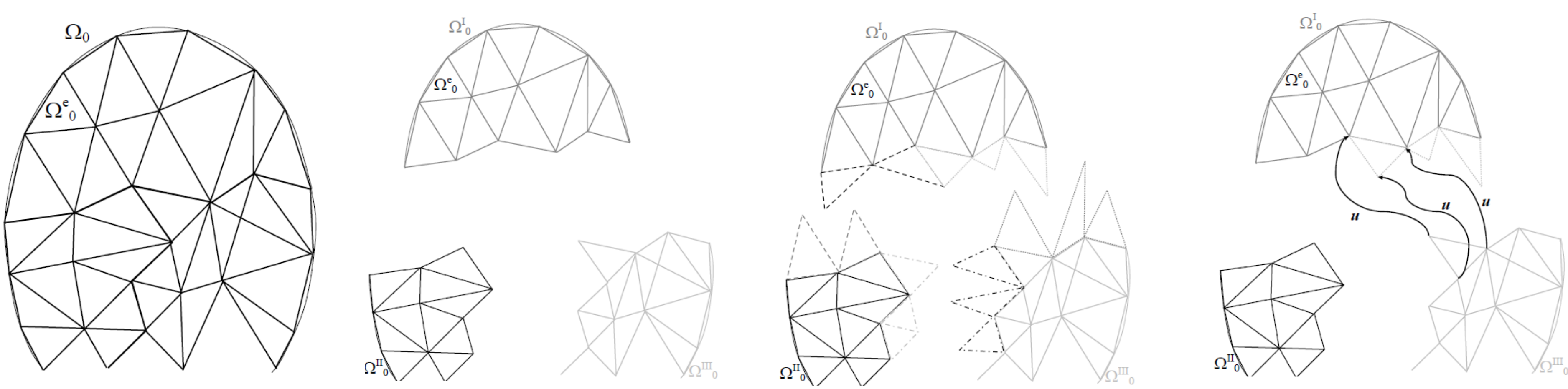

(a) Initial mesh (b) Partitioned mesh (c) Ghost elements (d) Communications

(Becker et al. 2012, Wu et al. 2013)

- Multi-scale study of the shear layer test
  - H = 1cm , 2cm, 4cm and 8cm
    in order to consider size effects
  - RVE size d = 0.2cm
  - Material law
    - Bulk modulus = 175 GPa
    - Shear modulus = 81 GPa
    - Yield stress = 507 MPa
    - Hardening modulus = 200 MPa

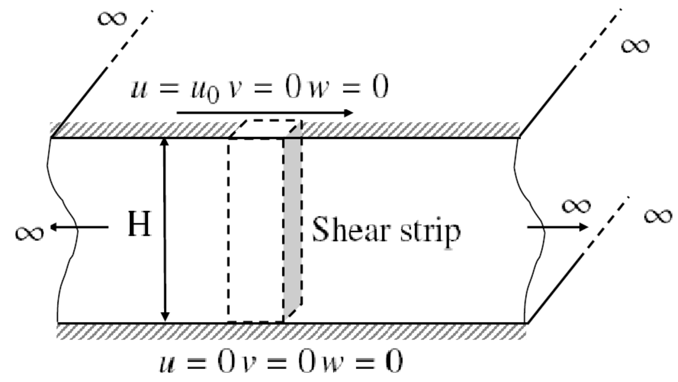

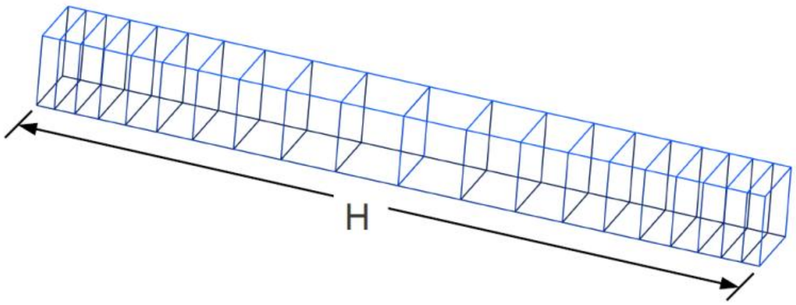

(a) Macroscopic mesh

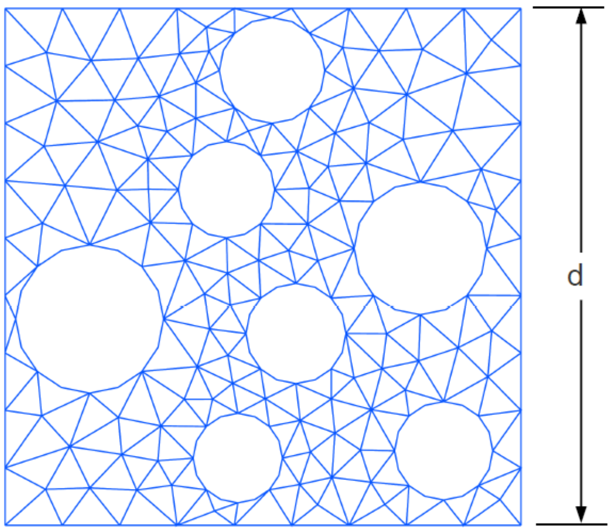

(b) Microscopic mesh

- Multi-scale study of the shear layer test (2)
  - Size effect

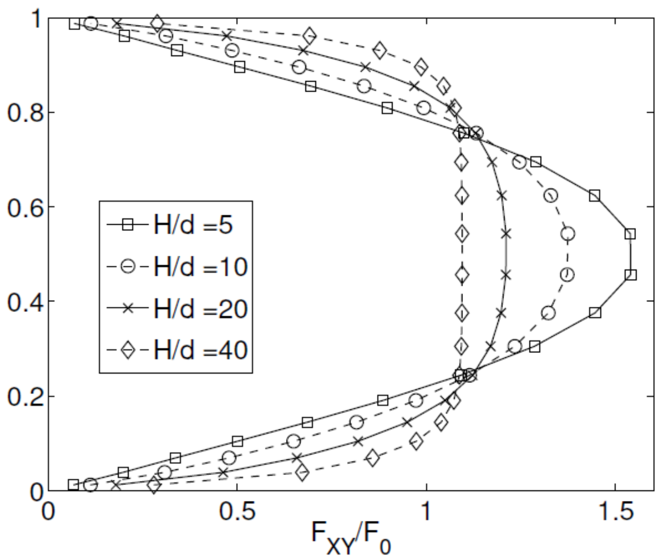

Deformation profile

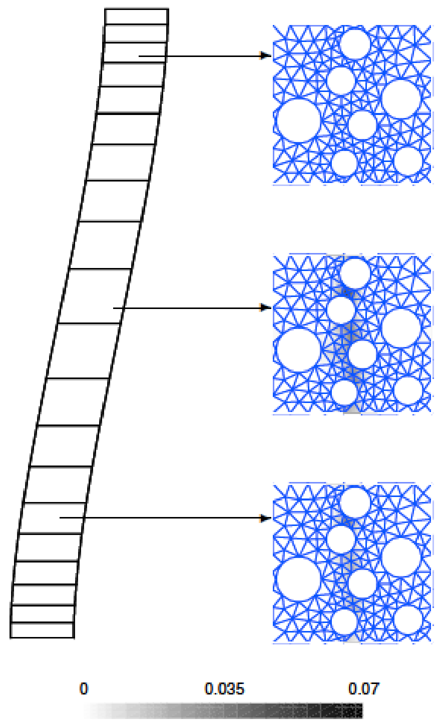

Deformed shape with H/d = 10

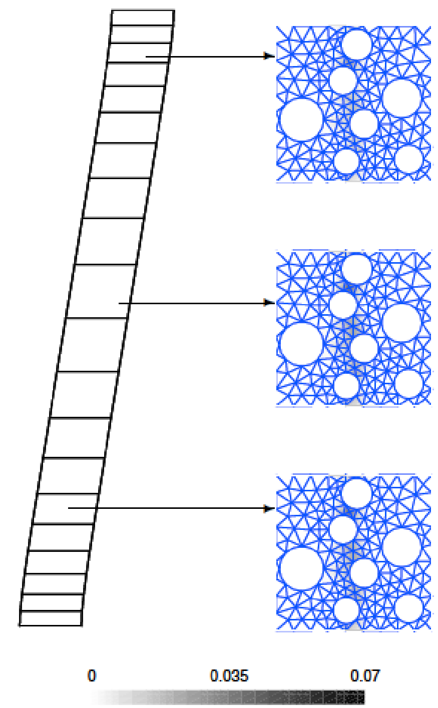

Deformed shape with H/d = 40

- Conclusions
  - The Mindlin strain gradient problems are solved using the discontinuous Galerkin formulations with conventional finite elements
  - The resulting one-field formulation can easily be implemented in existing software
  - This formulation is used for second-order multi-scale computational homogenizations
  - The micro and macro-scale problems consider finite strains
  - Size effects in heterogeneous elasto–plastic materials can be studied

Topics

- PBC enforcement based on the polynomial interpolation method

  (Nguyen, Geuzaine, Béchet & Noels CMS 2012)

- Second-order multi-scale computational homogenization scheme based on the Discontinuous Galerkin method (called second-order DG-based FE2 scheme)
  - DG method is used to solved the macroscopic Mindlin strain gradient
  - Usual FE
  - Parallel computation

  (Nguyen, Becker & Noels CMAME 2013)

- Use of this ***second-order DG-based FE^2 scheme*** to capture instabilities in cellular materials
  - Arc-length path following method is adopted at both scales because of the presence of the macroscopic localization and micro-buckling
  - Parallel computation

  (Nguyen & Noels IJSS 2014)

Université de Liège

- Microscopic classical continuum
  - Enforcement of PBC using the polynomial interpolation method
  - Arc-length path following method
- Macroscopic Mindlin strain gradient continuum
  - Resolution with Discontinuous Galerkin formulation
  - Arc-length path following method
- Full parallel computations
  - Macroscopic parallel distribution using ghost elements
  - Microscopic parallel distribution

- Why the arc-length path following method?
  - Load-based increments (pure load, arc-length increments, etc.) are preferred to improve the Newton-Raphson convergence
  - Presence of critical points (e.g. limit points) & unstable equilibrium paths for which the conventional Newton-Raphson method fails→ arc-length increments

- Path following method
  - Macro-scale problem
    - Path following with applied loading

$$\mathrm{a}\left(\bar{\mathbf{u}}, \delta\bar{\mathbf{u}}\right) = \bar{\mu}\mathrm{b}\left(\delta\bar{\mathbf{u}}\right)$$

    - Arc-length constraint

$$\bar{h}(\Delta\bar{\mathbf{u}}, \Delta\bar{\mu}) = \frac{\Delta\bar{\mathbf{u}}^T\Delta\bar{\mathbf{u}}}{\Psi^2} + \Delta\bar{\mu}^2 - \Delta L^2 = 0\,,$$

  - Micro-scale problems
    - Path following method on the applied boundary conditions

$$\tilde{\mathbf{C}}\tilde{\mathbf{u}}_b - \mathbf{g}\left(\bar{\mathbf{F}}, \bar{\mathbf{F}}\otimes\boldsymbol{\nabla}_0\right) = \mathbf{0}$$

$$\left(\bar{\mathbf{F}}, \bar{\mathbf{F}}\otimes\boldsymbol{\nabla}_0\right) = \left(\bar{\mathbf{F}}, \bar{\mathbf{F}}\otimes\boldsymbol{\nabla}_0\right)_0 + \mu\left[\left(\bar{\mathbf{F}}, \bar{\mathbf{F}}\otimes\boldsymbol{\nabla}_0\right)_1 - \left(\bar{\mathbf{F}}, \bar{\mathbf{F}}\otimes\boldsymbol{\nabla}_0\right)_0\right]$$

    - Arc-length constraint

$$h(\Delta\mathbf{u}, \Delta\mu) = \frac{\Delta\mathbf{u}^T\Delta\mathbf{u}}{\psi^2} + \Delta\mu^2 - \Delta l^2 = 0$$

    - Compute by increments until $\mu = 1$

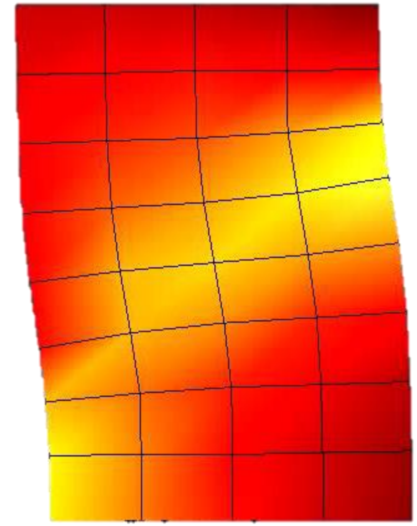

$\bar{\mathbf{P}}, \bar{\mathbf{Q}}$

$\left(\bar{\mathbf{F}}, \bar{\mathbf{F}}\otimes\boldsymbol{\nabla}_0\right)_1$

$\frac{\partial\bar{\mathbf{P}}}{\partial\bar{\mathbf{F}}}, \frac{\partial\bar{\mathbf{P}}}{\partial\bar{\mathbf{F}}\otimes\boldsymbol{\nabla}_0}$

$\frac{\partial\bar{\mathbf{Q}}}{\partial\bar{\mathbf{F}}}, \frac{\partial\bar{\mathbf{Q}}}{\partial\bar{\mathbf{F}}\otimes\boldsymbol{\nabla}_0},$

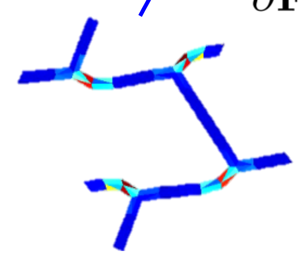

- Compression of an hexagonal honeycomb plate
  - Plate: H = 102 mm, L = 65.8mm
  - Honeycomb: l = 1mm, t = 0.1 mm
  - Elasto-plastic material
    - Bulk modulus = 67.55 GPa
    - Shear modulus = 25.9 GPa
    - Initial yield stress = 276 MPa

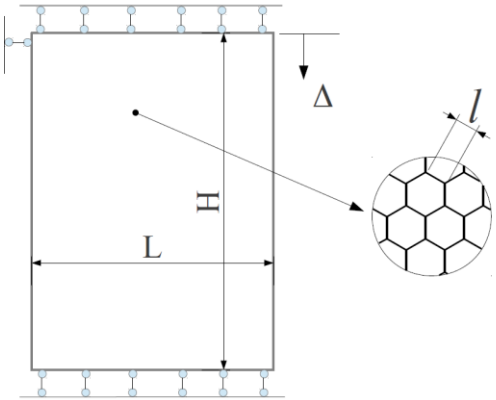

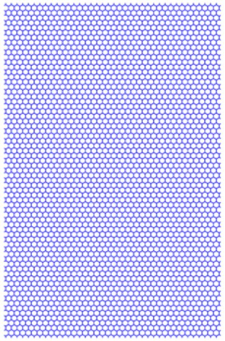

Full model

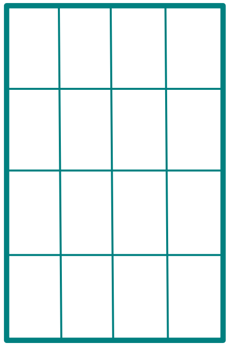

Mesh 0

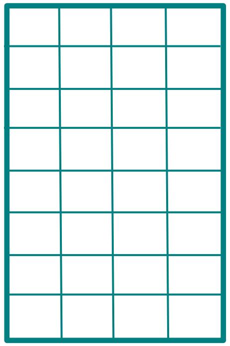

Mesh 1

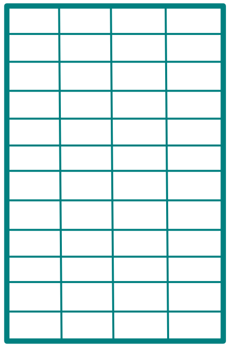

Mesh 2

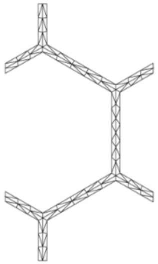

Unit cell mesh

- Compression of an hexagonal honeycomb plate (2)
  - Captures the softening onset
  - Captures the softening response
  - No macro-mesh size effect

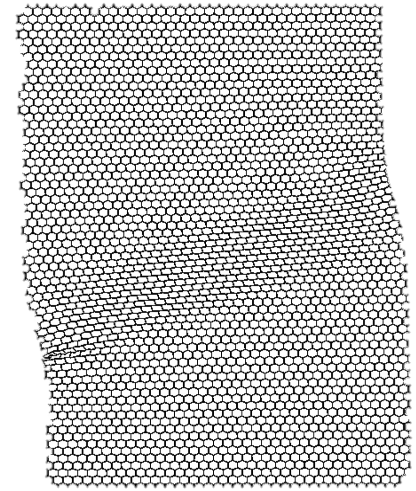

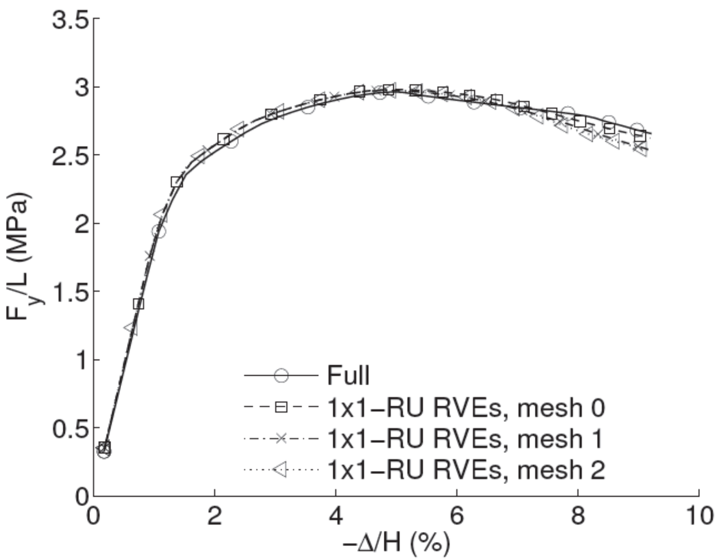

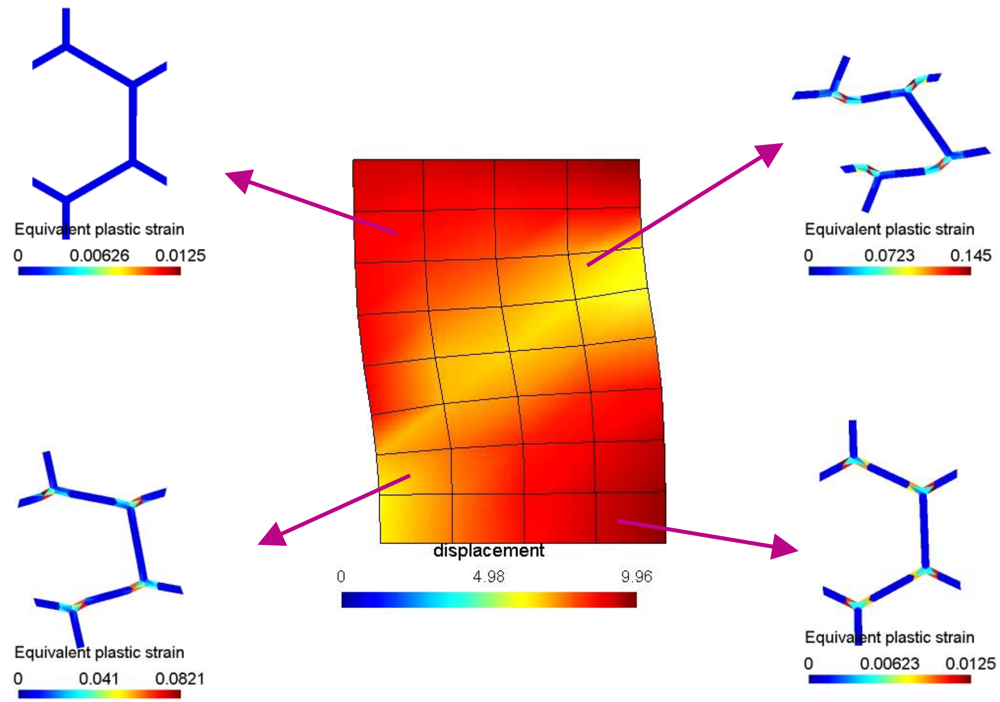

- Compression of an hexagonal honeycomb plate (3)
  - Influence of cell size
    - Same honeycomb structure: l = 1mm, t = 0.1 mm
    - Different plate dimensions

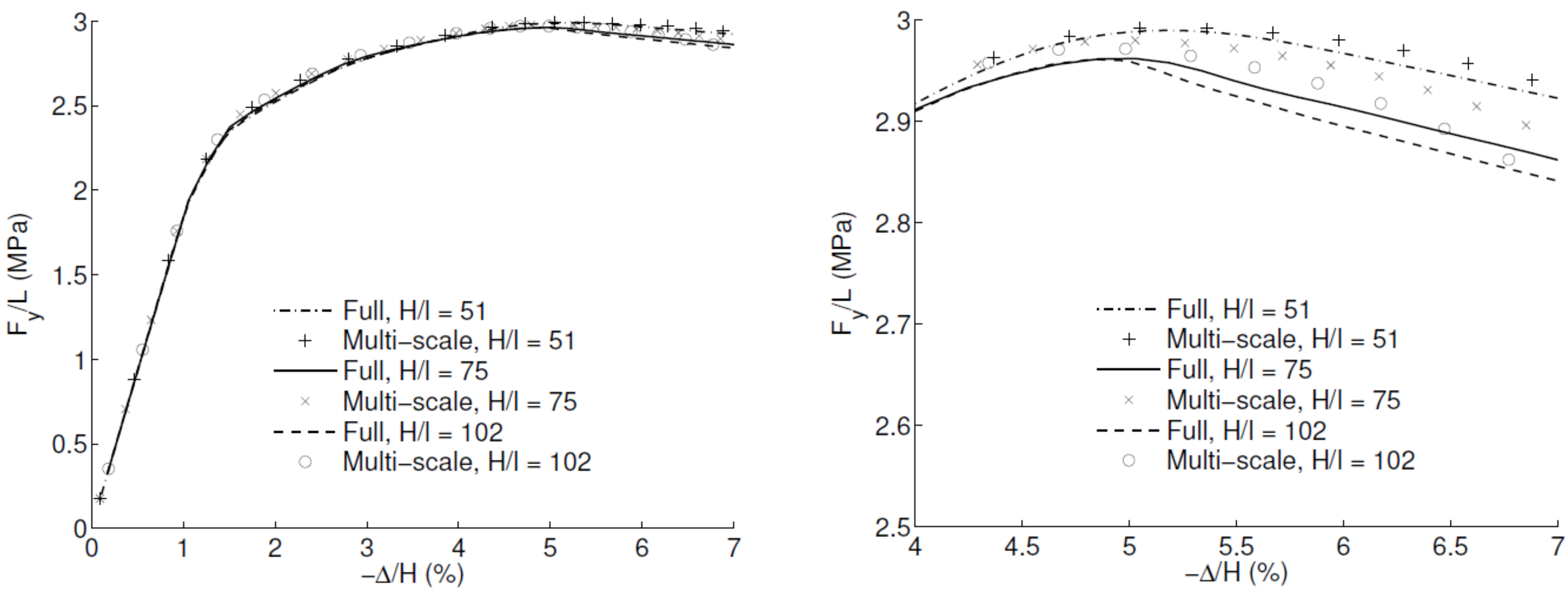

(a) overall response

(b) zoom at the strain softening onset

- Compression of a hexagonal honeycomb plate with a centered hole
  - Central radius: r = 15mm
  - Honeycomb: l = 1mm, t= 0.1mm
  - Elasto-plastic material
    - Bulk modulus = 67.55 GPa
    - Shear modulus = 25.9 GPa
    - Initial yield stress = 276 MPa

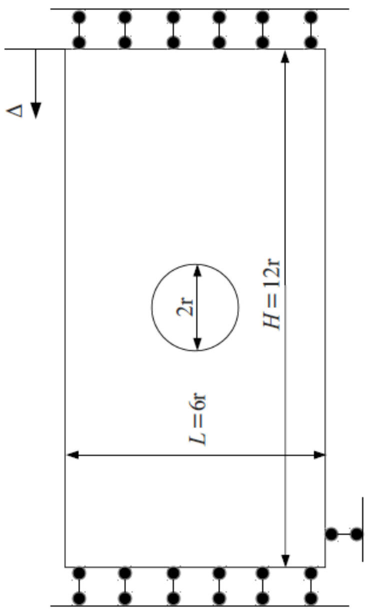

Geometry & BCs

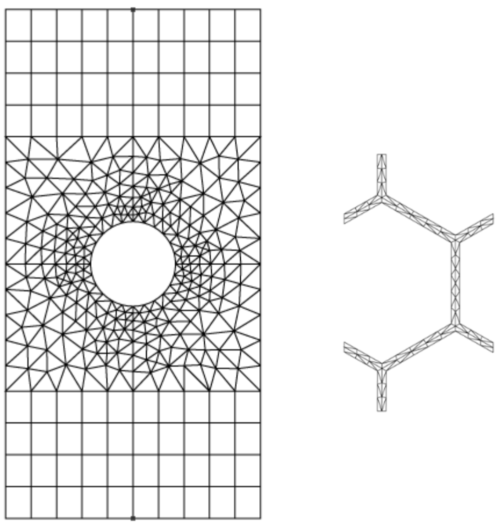

Multi-scale model

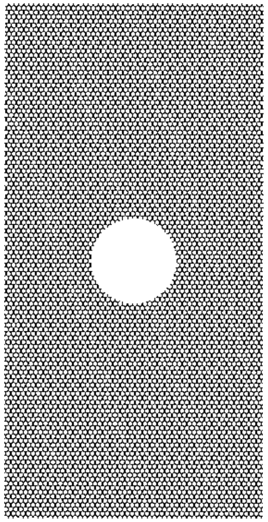

Full model with 300.000 quadratic triangles

- Compression of a hexagonal honeycomb plate with a centered hole (2)
  - Results given by full and multi-scale models are comparable

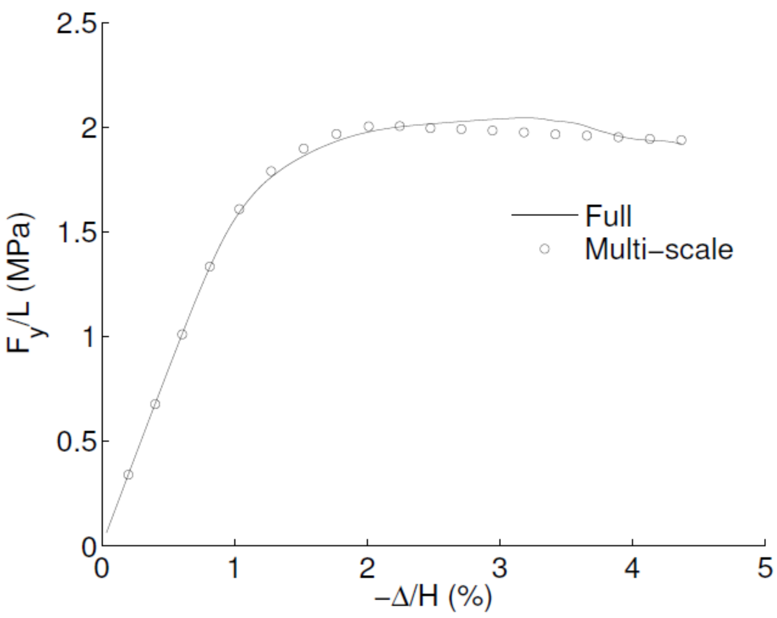

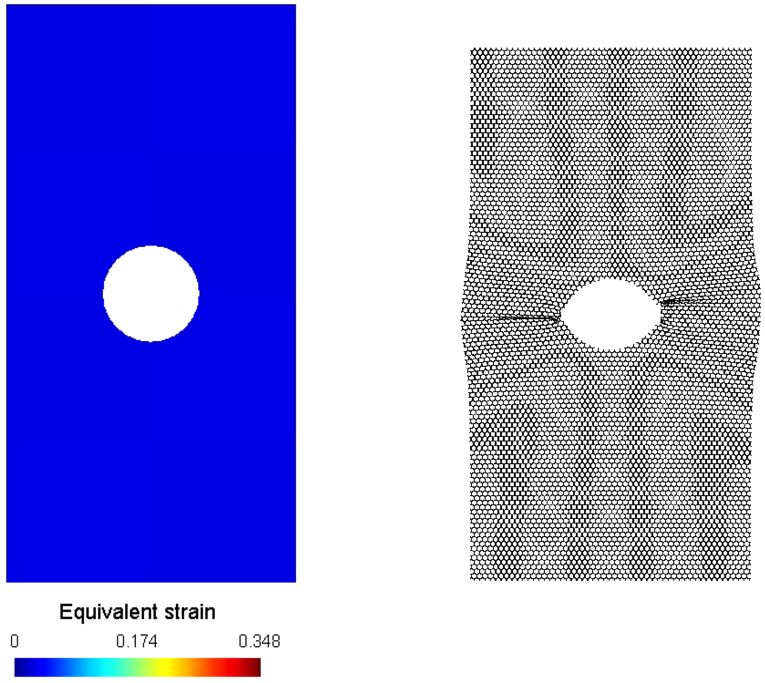

- A second-order DG-based FE^2 scheme was developed with the following novelties:
  - The periodic boundary condition is enforced using the polynomial interpolation method without the need of conforming meshes
  - The macroscopic Mindlin strain gradient problem is solved using the Discontinuous Galerkin method with conventional finite elements
  - The arc-length path following method is applied at both scales to capture their instabilities

Current works

- Polypropylene foam
  - Experimental tests (F. Wan)

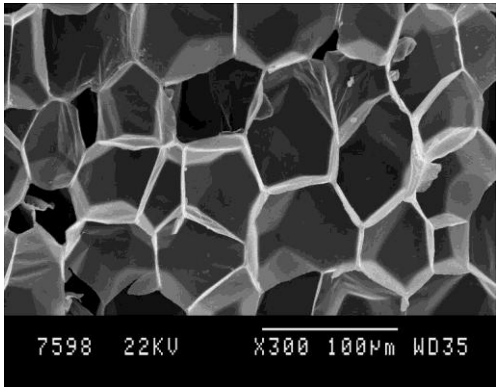

SEM image of a PP foam with 4% CNTs

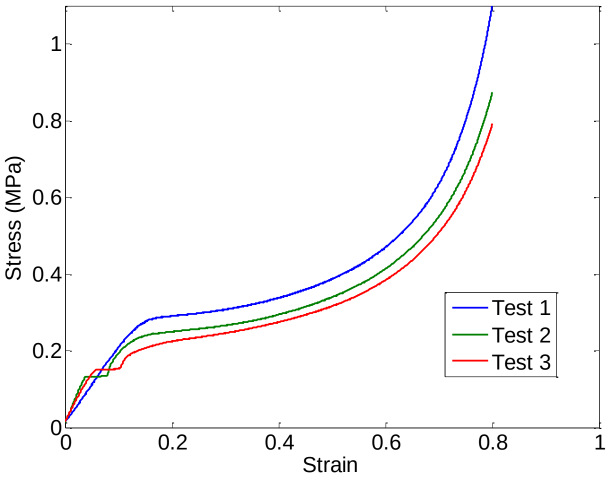

- Imperfections→ reduce the stiffness
  - Random cell sizes and shapes
  - Non-uniform distribution of solid materials of cell walls
  - Curvature of cell walls
  - Loss of cell walls
  - Corrugation of cell walls
  - Fracture of cell walls
  - ...

- Homogenized properties based on the tetrakaidecahedron unit cell
  - Ideal unit cell models

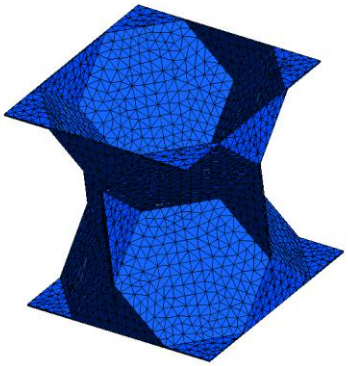

Closed unit cell

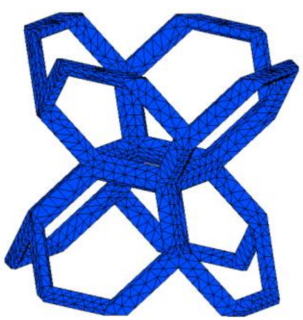

Open unit cell

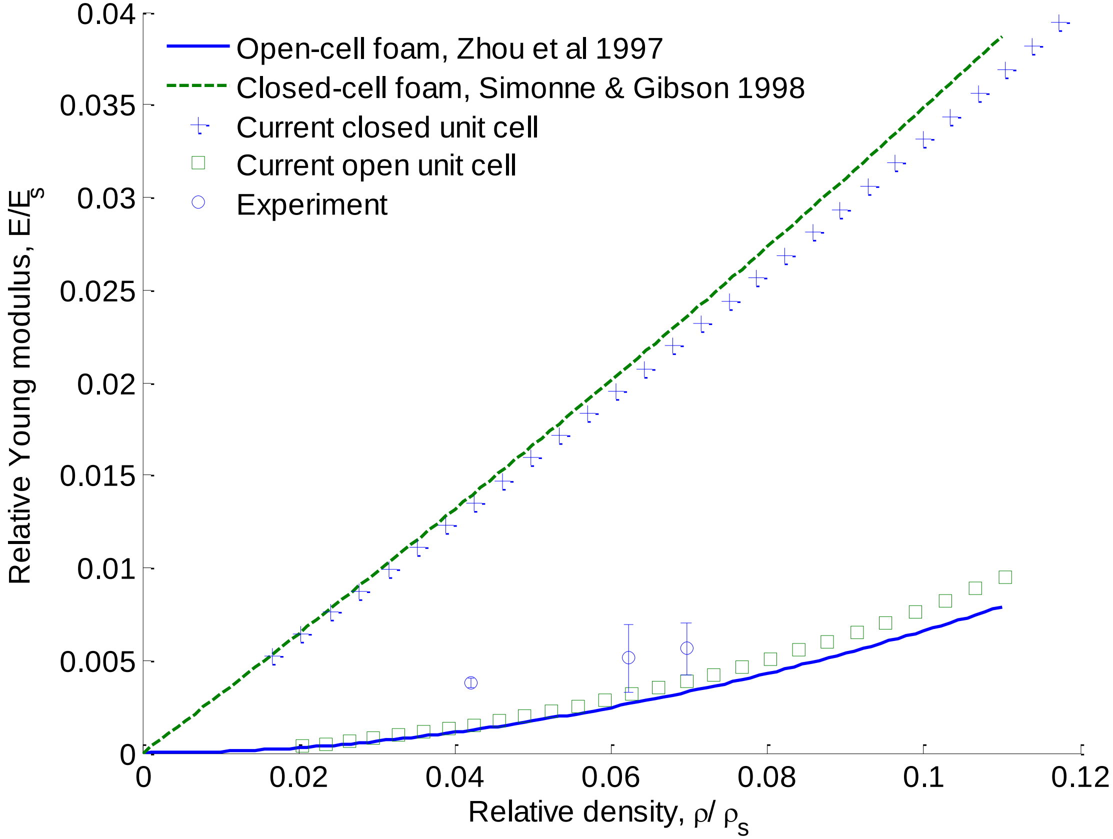

→imperfections must be considered

- Homogenized properties based on the tetrakaidecahedron unit cell (2)
  - Unit cell with mass concentration at cell edges
    - Mass concentration parameter: **ϕ=** mass at cell edge/ total mass

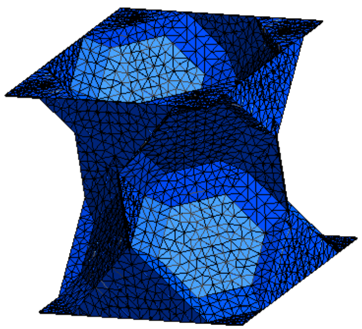

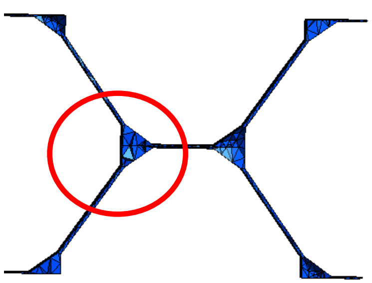

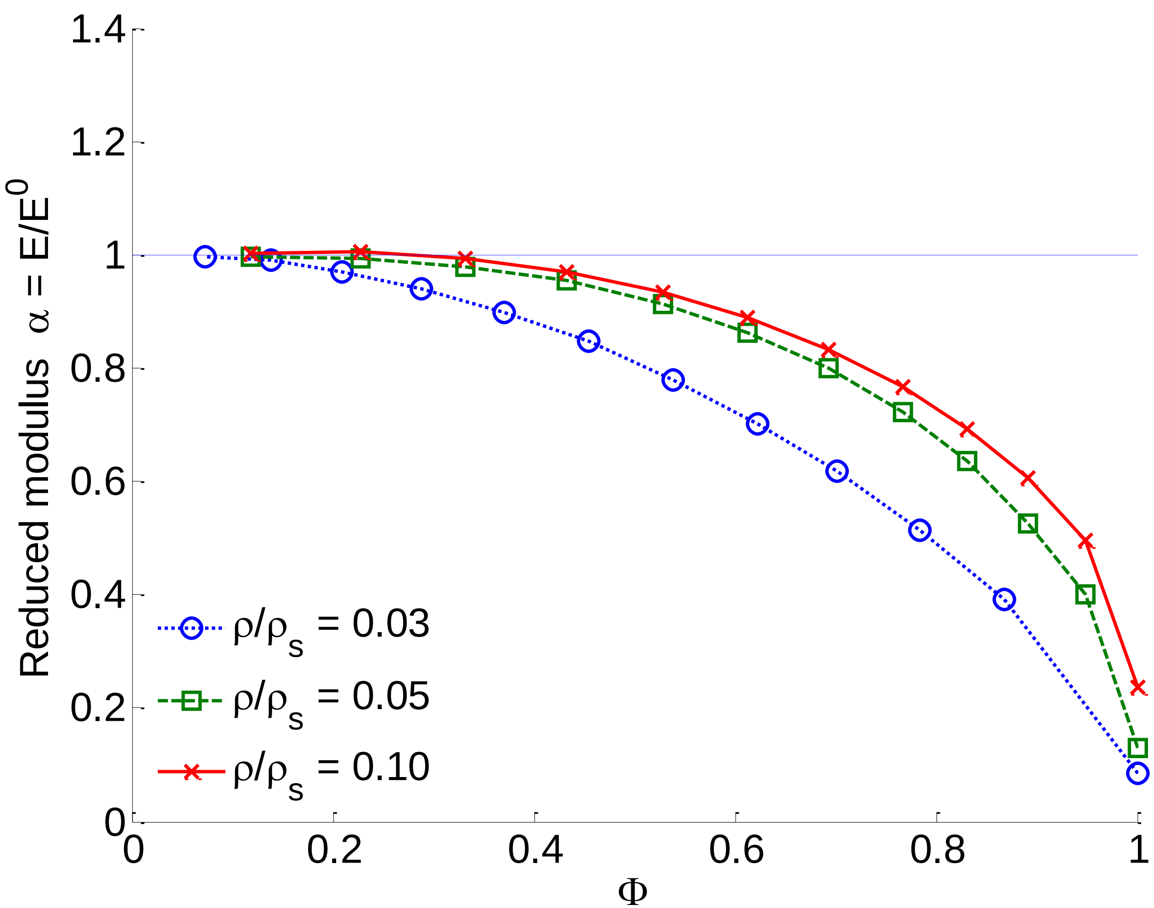

- Experimental validation in the context of the ARC project with the RVE meshes coming from tomographical images of the microstructure

- Electromagnetic-mechanical coupling problems since electromagnetic properties are modified during the mechanical loading (as the shape is deformed)

- Discontinuous-continuous schemes for sharper localization problems following the works of Massart et al. 2007, Nguyen et al. 2011 or Coenen et al. 2012

- Material tailoring with required properties by computational homogenization schemes

- …

Thank you for your attention!

Annex 1 - Macro-scale path following resolution

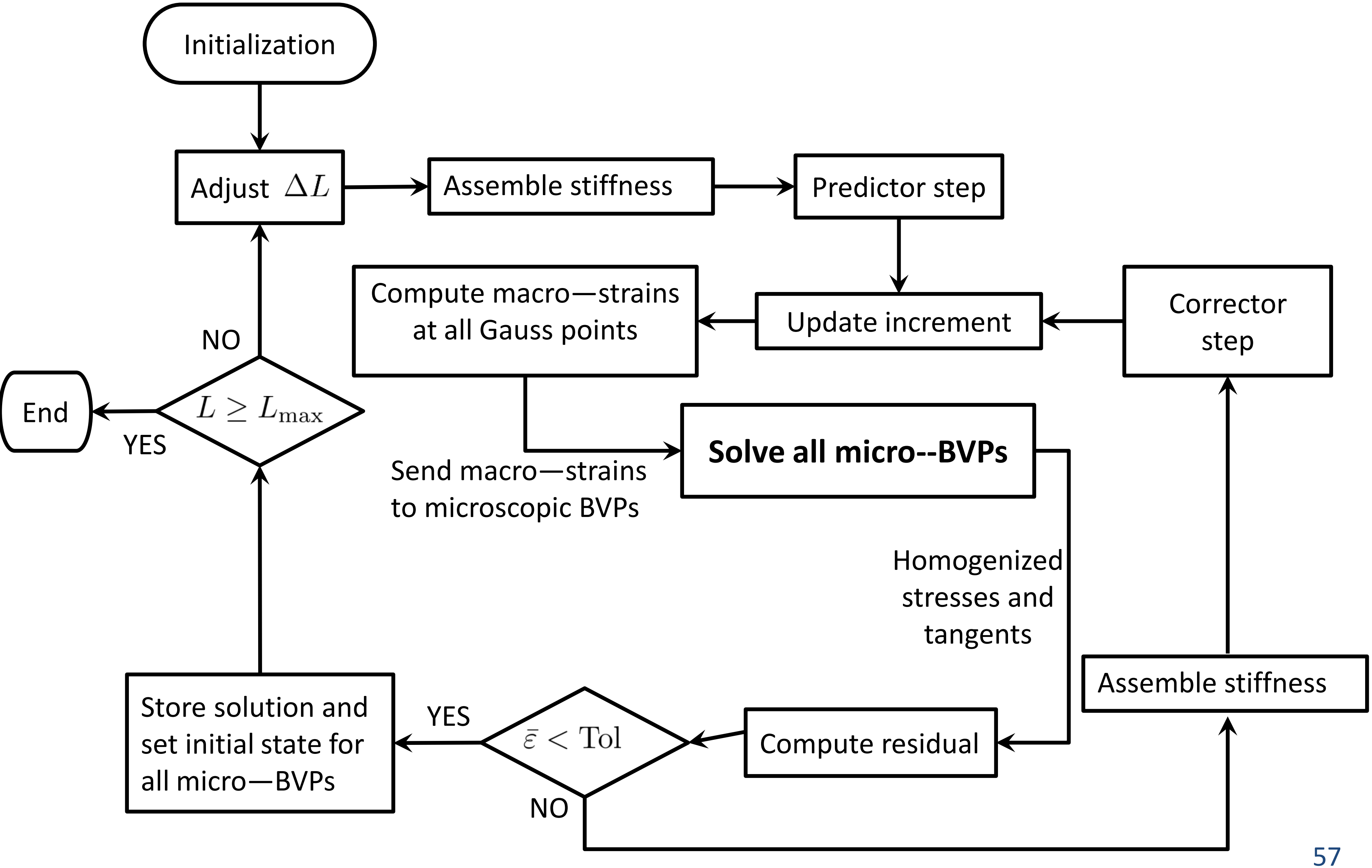

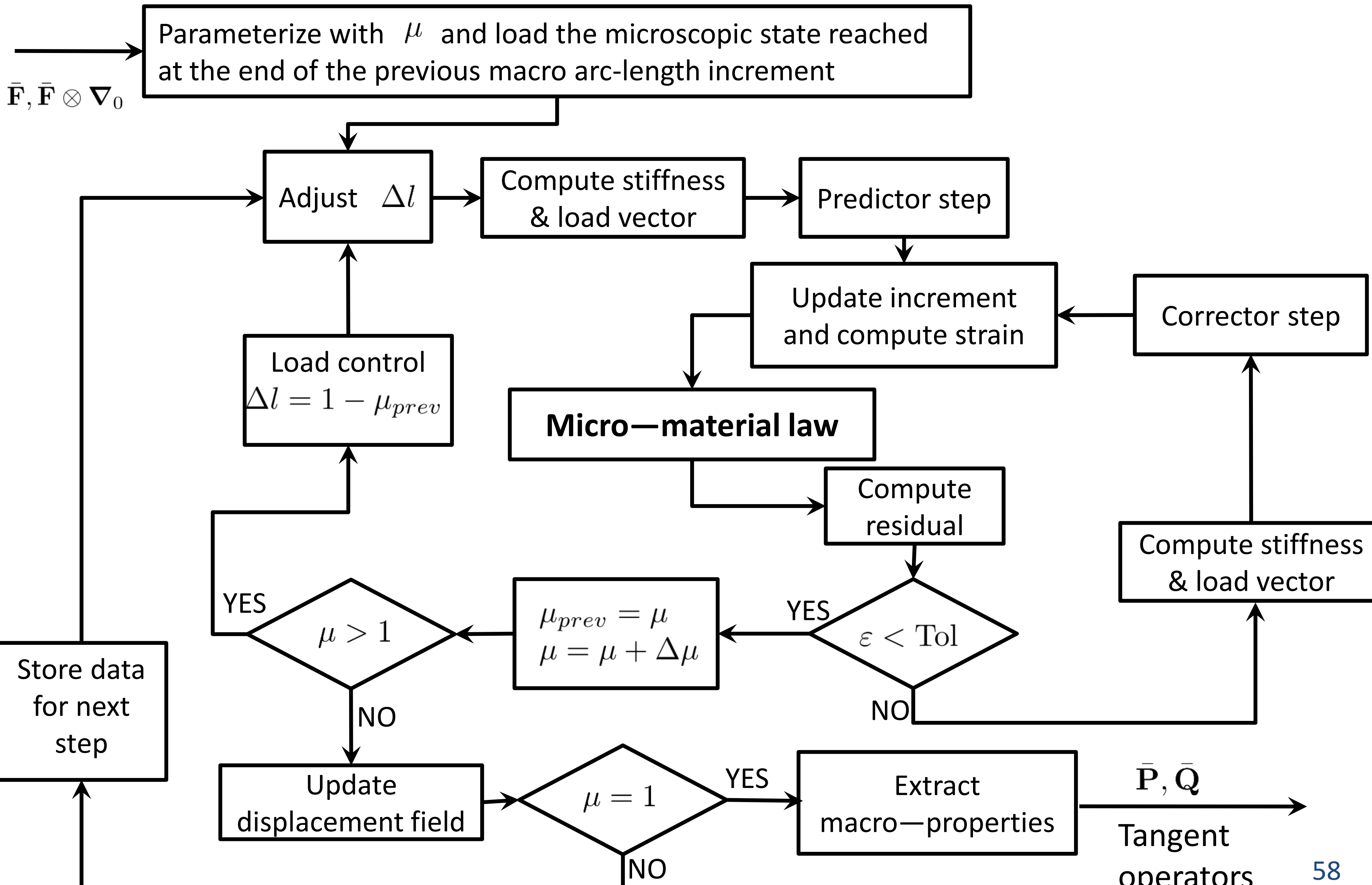
$\bar{\mathbf{F}}, \bar{\mathbf{F}} \otimes \boldsymbol{\nabla}_0$
Parameterize with μ and load the microscopic state reached at the end of the previous macro arc-length increment
Adjust Δl
Compute stiffness & load vector
Predictor step
Update increment and compute strain
Corrector step
Load control $\Delta l = 1 - \mu_{prev}$
Micro—material law
Compute residual
Compute stiffness & load vector
YES
$\mu > 1$
$\mu_{prev} = \mu$
$\mu = \mu + \Delta\mu$
YES
$\varepsilon < \mathrm{Tol}$
NO
Store data for next step
NO
Update displacement field
$\mu = 1$
YES
Extract macro—properties
$\bar{\mathbf{P}}, \bar{\mathbf{Q}}$
Tangent operators
NO

Annex 3 – Computation time

Method	CPU time per iteration	Used memory
Full model	92 seconds	5.6 gigabytes
Multi–scale model, mesh 0	36 seconds	1.3 gigabytes
Multi–scale model, mesh 1	84 seconds	2.6 gigabytes
Multi–scale model, mesh 2	146 seconds	4.0 gigabytes

Computation time and used memory of the full model and multi–scale models. These computations were performed in the same machine with one processor